SEMIANNUAL REPORT NO. 3

DEVELOPMENT OF MAIN-SHAFT SEALS
FOR ADVANCED AIR-BREATHING
PROPULSION SYSTEMS
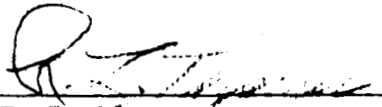
Prepared for

NATIONAL AERONAUTICS AND SPACE ADMINISTRATION
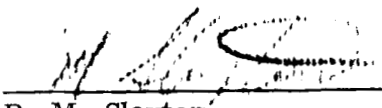
January 20, 1967

CONTRACT NAS3-7609

Prepared by: _____
R. L. Thomas
Assistant Project Engineer

_____
A. J. Parks
Assistant Project Engineer

_____
R. M. Slayton
Project Manager

Approved by: _____
R. P. Shevchenko
Senior Project Engineer

Pratt & Whitney Aircraft   DIVISION OF UNITED AIRCRAFT CORPORATION

U
A®

PREFACE

This report describes the progress of work conducted between 1 July 1966 and 31 December 1966 by the Pratt & Whitney Aircraft Division of United Aircraft Corporation, East Hartford, Connecticut on Contract NAS3-7609, Development of Main-Shaft Seals for Advanced Air-Breathing Propulsion Systems, for the Lewis Research Center of the National Aeronautics and Space Administration.

Richard M. Slayton is Project Manager for Pratt & Whitney Aircraft for this program.

The following National Aeronautics and Space Administration personnel have been assigned to this project.

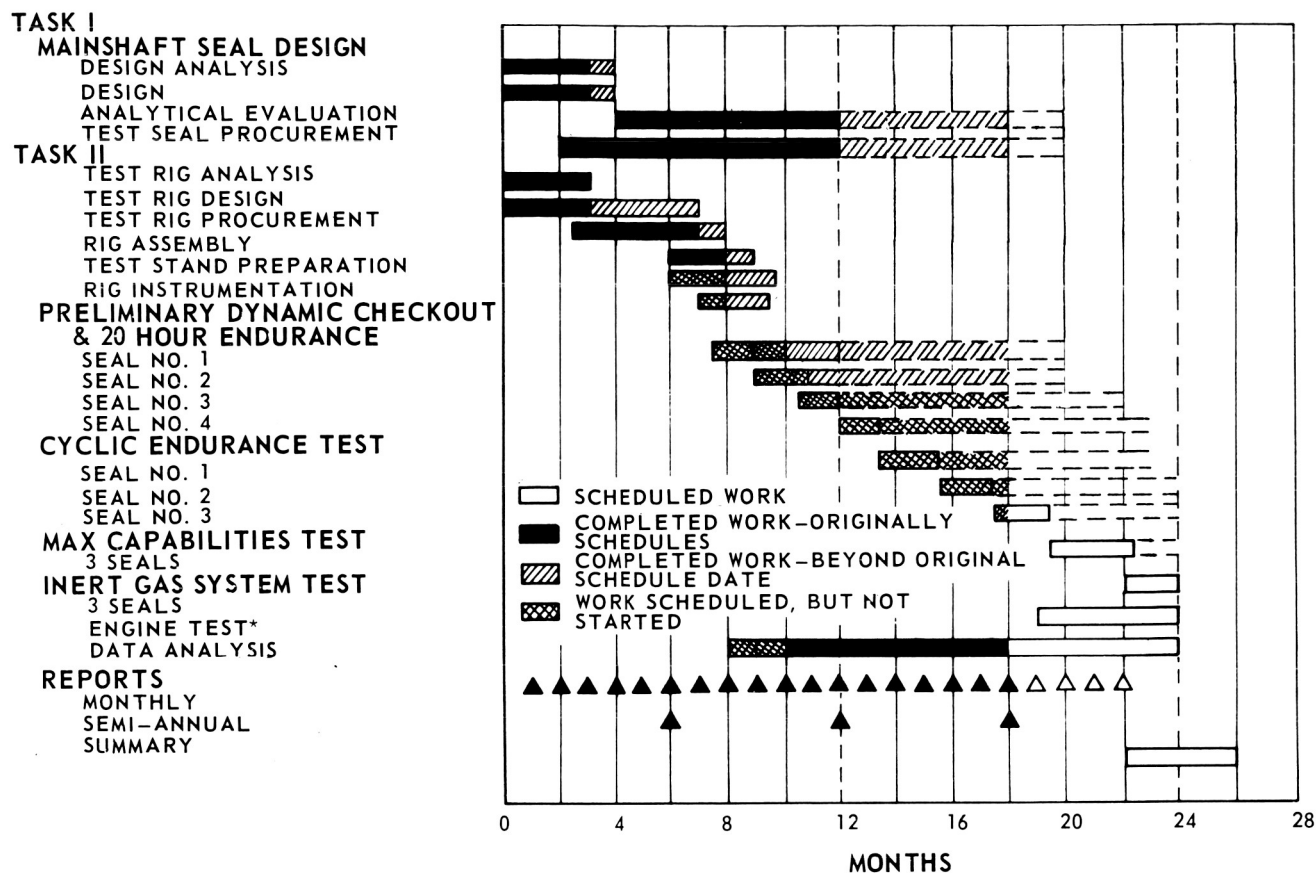|	
Contracting Officer	J. H. DeFord
Contract Administrator	T. J. Charney
Project Manager	D. P. Townsend
Research Advisor	L. P. Ludwig

SUMMARY

This report covers the work accomplished during the third six-month period (July 1966 through December 1966) of the NAS3-7609 contract which was initiated 29 June 1965 and extends for a total of 24 months.

Briefly, the objective of the work to be accomplished is to analyze, design, procure, and test four types of main-shaft seals for advanced gas-turbine applications.

A program summary is presented in Figure 1. The work accomplished during this six-month period is outlined below.

1.   Contacts with vendors were continued in relation to the seals to be evaluated.

2.   Detailed analytical studies of all seal configurations were continued.

3.   Approval was received from NASA for the last seal concept to be evaluated. This was the externally pressurized hydrostatic seal.

4.   Procurement of all types of seals to be evaluated was started and all but the face contact seal with bellows secondary seal have been received.

5.   Builds numbers 2 through 6 of the face contact seal with piston ring secondary seal were completed, and tests were run at simulated engine conditions (200 to 400 ft/sec rubbing surface speed with air temperatures from ambient to 1200°F and with oil at 250°F).

6.   Builds numbers 1 through 7 of the orifice-compensated hydrostatic seal were completed. Preliminary dynamic testing resulted in rubbing and excessive leakage with the greater amount of rubbing occurring on the inner seal lip. This indicates that the seal components were not parallel when the rub occurred.

7.   The instrumentation validation rig was used in the development of the carbon wear and the seal torque-measuring instrumentation.

TASK I
  MAINSHAFT SEAL DESIGN
    DESIGN ANALYSIS
    DESIGN
    ANALYTICAL EVALUATION
    TEST SEAL PROCUREMENT
TASK II
    TEST RIG ANALYSIS
    TEST RIG DESIGN
    TEST RIG PROCUREMENT
    RIG ASSEMBLY
    TEST STAND PREPARATION
    RIG INSTRUMENTATION
  PRELIMINARY DYNAMIC CHECKOUT
    & 20 HOUR ENDURANCE
    SEAL NO. 1
    SEAL NO. 2
    SEAL NO. 3
    SEAL NO. 4
  CYCLIC ENDURANCE TEST
    SEAL NO. 1
    SEAL NO. 2
    SEAL NO. 3
  MAX CAPABILITIES TEST
    3 SEALS
  INERT GAS SYSTEM TEST
    3 SEALS
    ENGINE TEST*
    DATA ANALYSIS
  REPORTS
    MONTHLY
    SEMI-ANNUAL
    SUMMARY

Legend:
- ☐ SCHEDULED WORK
- ■ COMPLETED WORK–ORIGINALLY SCHEDULES
- ▨ COMPLETED WORK–BEYOND ORIGINAL SCHEDULE DATE
- ▧ WORK SCHEDULED, BUT NOT STARTED

MONTHS: 0 4 8 12 16 20 24 28

* CONTINGENT UPON PERFORMANCE OF SEAL AND AVAILABILITY OF ENGINE
  FOR TESTING. SEE LETTER OF TRANSMITTAL DATED FEB. 26, 1965.

Figure 1   Main Shaft Seal Program Summary

SEMIANNUAL REPORT NO. 3

DEVELOPMENT OF MAIN-SHAFT SEALS
FOR ADVANCED AIR BREATHING
PROPULSION SYSTEMS

by

R. L. Thomas, A. J. Parks, and R. M. Slayton

ABSTRACT

Four main-shaft seals for advanced gas-turbine applications have been designed and are being analyzed and tested. The seals being studied are an orifice-compensated hydrostatic face seal, an externally pressurized hydrostatic face seal, a carbon-face-contact seal with a bellows secondary seal, and a carbon-face-contact seal with a piston-ring secondary seal. During the report period, Builds 2 through 6 of the face seal with piston-ring secondary seal and Builds 1 through 7 of the orifice-compensated hydrostatic seal were tested. In addition, development testing on instrumentation to measure carbon seal wear and seal torque was conducted.

TABLE OF CONTENTS

LIST OF ILLUSTRATIONS

LIST OF ILLUSTRATIONS (Cont'd)

LIST OF ILLUSTRATIONS (Cont'd)

LIST OF ILLUSTRATIONS (Cont'd)

LIST OF ILLUSTRATIONS (Cont'd)

LIST OF ILLUSTRATIONS (Cont'd)

LIST OF TABLES

I. INTRODUCTION

The objective of the program established by Contract NAS3-7609 is to analyze, design, and test four types of main-shaft seals for advanced, air-breathing, propulsion systems. Test effort is being directed toward:

1. Determining the characteristics of improved main-shaft seals;

2. Establishing acceptable operational limits for such seals in terms of temperature, speed, and pressure differential; and

3. Establishing a measure of reliability (wear and stability) for such seals.

This report discusses the analytical design and test efforts conducted during the third six-month period of the contract.

II. DISCUSSION

A. TASK I – MAIN-SHAFT SEAL DESIGN

1. INTRODUCTION

Task I of Exhibit A of the contract specifies that the Contractor shall design and analyze one seal assembly of each of the following four types:

1. An orifice-compensated, hydrostatic, face seal;

2. An externally pressurized, hydrostatic (floating face) seal;

3. A carbon face-contact seal with a bellows secondary seal; and

4. A carbon face-contact seal with a piston-ring secondary seal.

The seals were required to be capable of operating at the following conditions:

Seal Sliding Speed	0 to 500 ft/sec.
Seal Pressure Differential	0 to 300 psi
Gas Temperature	Ambient to 1300°F
Oil Sump Temperature	Ambient to 500°F

Four seal assemblies have been designed to meet the contractual specifications. The first three types of seals listed above were designed by the Stein Seal Company and were discussed in the second semiannual report (PWA-2879). The last type was designed by Pratt & Whitney Aircraft and was discussed in the first semiannual report (PWA-2683). The seal design characteristics are summarized in Table I.

TABLE I

MAIN-SHAFT SEAL CHARACTERISTICS

Seal Designation	Film Riding	Orifice Compensated	Single Piston Ring Secondary	Double Piston Ring Secondary	Bellows Secondary	Capable of Being Externally Pressurized
A (Stein)	X	X	X			
B (Stein)	X	X		X		X
C (Stein)					X	X
P&WA Design				X		

A	Orifice compensated hydrostatic face seal
B	Externally pressurized orifice compensated hydrostatic face seal
C	Face contact with bellows secondary
PWA	Face contact with piston ring secondary

During the current report period, detailed deflection analyses were performed for the three Stein-designed seals and the thermal analysis for the Pratt & Whitney Aircraft-designed seal was modified to account for the transfer of energy which bypasses the oil passages in the seal plate. Subsequently, a thermal analysis of the carbon face-contact seal with piston ring secondary seal was performed.

2. DEFLECTION ANALYSIS

a. ORIFICE-COMPENSATED HYDROSTATIC FACE SEAL

The seal housing, seal plate deflection analysis for the orifice-compensated hydrostatic face seal was based on the work of R. T. Roark*. For analysis, the seal is considered to be composed of three sections, as shown in Figure 2. Section A is assumed to be a thick-walled cylinder exposed to a uniform internal and external radial pressure; section B is assumed to be a thick-walled cylinder exposed to a uniform internal pressure; and section C is assumed to be a ring fixed at the inner edge and uniformly loaded. Pertinent dimensions are shown in Figure 3.
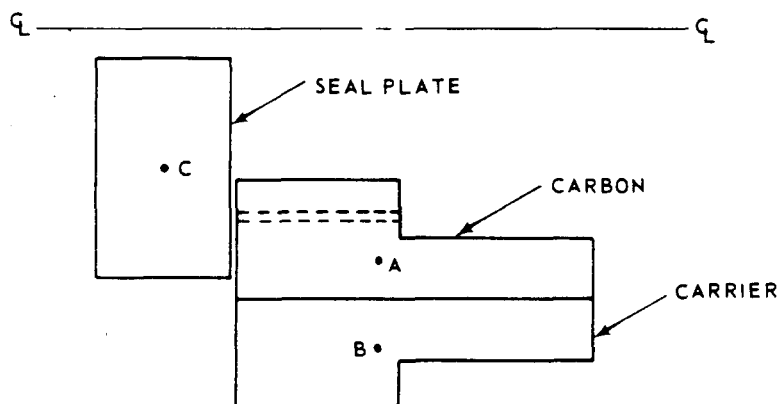
Figure 2   Analytical Sections of Orifice-Compensated Hydrostatic Face Seal

The radial deflection of the carbon is represented by the following equation from Roark.

$$\delta_A = \frac{P_1(b)}{E_1} \frac{2a^2}{b^2 - a^2} - \frac{P_o(b)}{E_1} \left(\frac{a^2 + b^2}{b^2 - a^2} - v_1 \right) \tag{1}$$

---

*R. T. Roark, Formulas for Stress and Strain, McGraw-Hill, New York, 1954
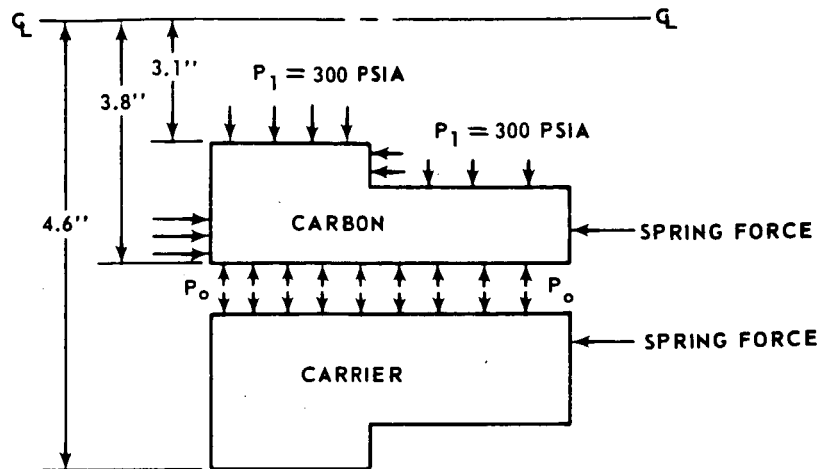
Figure 3   Dimensions and Loading for Orifice-Compensated Hydrostatic Face
            Seal Analysis

where:

P_1 = 300 psia

E_1 = 3.0×10^6 (Young's modulus of elasticity for carbon)

v_1 = 0.25 (Poissons ratio)

a = 3.1 in.

b = 3.8 in.

The radial deflection of the carrier is represented by:

$$\delta_B = \frac{P_o(b)}{E_2} \left(\frac{b^2 + c^2}{c^2 - b^2} + V_2 \right) \tag{2}$$

where:

E_2 = 30×10^6 (Young's modulus of elasticity for steel)

c = 4.6 in.

The deflections of the carbon and carrier are equal to ensure continuity of
structure. Therefore,

$$\delta_A = \delta_B \tag{3}$$

and P_o can be determined (for a press fit) to be 225.9 psia. Consequently,

$$\delta_A = \delta_B = 0.00016 \text{ in} \tag{4}$$

The pertinent dimensions for the seal plate are shown in Figure 4. This section is considered to be a ring fixed at its inner edge and uniformly loaded (Figure 5).
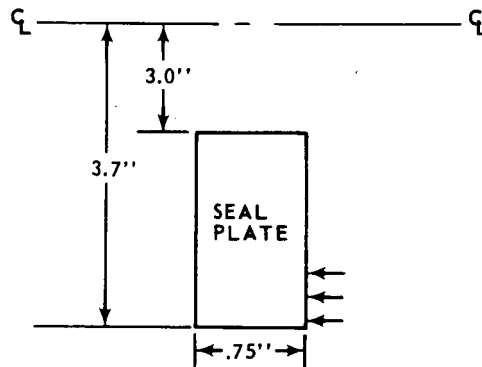
Figure 4   Dimensions for Orifice-Compensated Hydrostatic Face Seal Plate Analysis
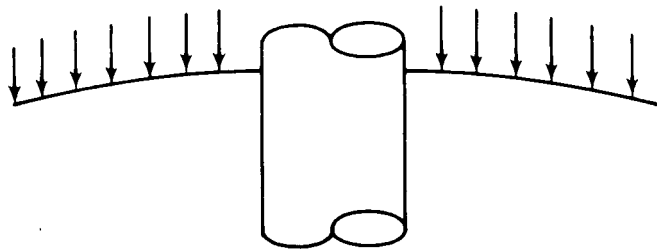
Figure 5   Analytical Model of Seal Plate

The equation for bending (from Roark) is:

$$y_B = \frac{\alpha w a^4}{E t^3} \tag{5}$$

where:

α = 0.00372 constant that is geometry dependent
w = 300 psi
a = 3.7 in.
E = 30×10^6 (Young's modulus of elasticity for steel)
t = 0.75 in.

Hence,

$$y_B = 0.000017 \text{ in.} \tag{6}$$

For shear, the equation is

$$y_s = \frac{0.375 \, w \, a^2}{tG} \left[2 \ln \alpha - 1 + \frac{1}{\alpha^2} \right] \tag{7}$$

where:

α = 1.23 = outer radius/inner radius

G = 12×10^6 = shear modulus

Substituting the appropriate values yields

$$y_s = 0.0000125 \text{ in.} \tag{8}$$

Consequently, the total deflection (neglecting bending and shear caused by loading on the outer edge) is

$$y_t = 0.0000295$$

Geometric similarities tend to eliminate angular misalignment in the carbon and carrier. The total deflection of the seal plate interference with the seal-carrier is shown in Figure 6.
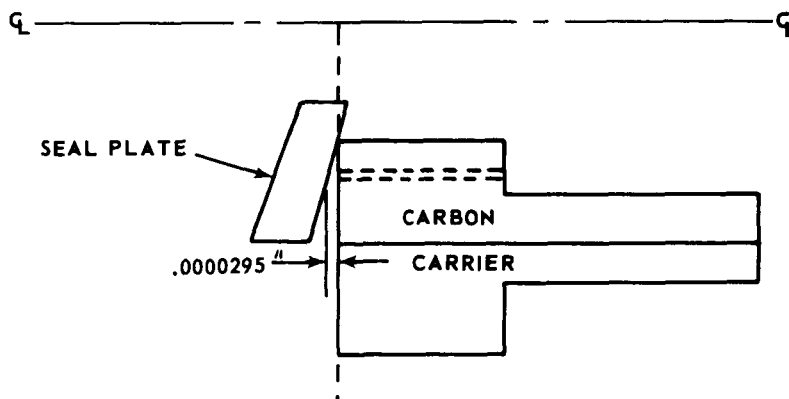
Figure 6   Deflection of Seal Plate in Orifice-Compensated Hydrostatic Face

b. <u>EXTERNALLY PRESSURIZED HYDROSTATIC SEAL</u>

The externally pressurized hydrostatic seal was assumed to consist of four parts plus the seal plate for the purpose of analysis, as shown in Figure 7. The seal plate for this seal is essentially the same as that of the orifice-compensated hydrostatic face seal, and, therefore, the analytical results are the same. Analysis of the remainder of the seal has been started. The procedure has been determined and a computer program has been written to solve the equations simultaneously for the resultant deflections.
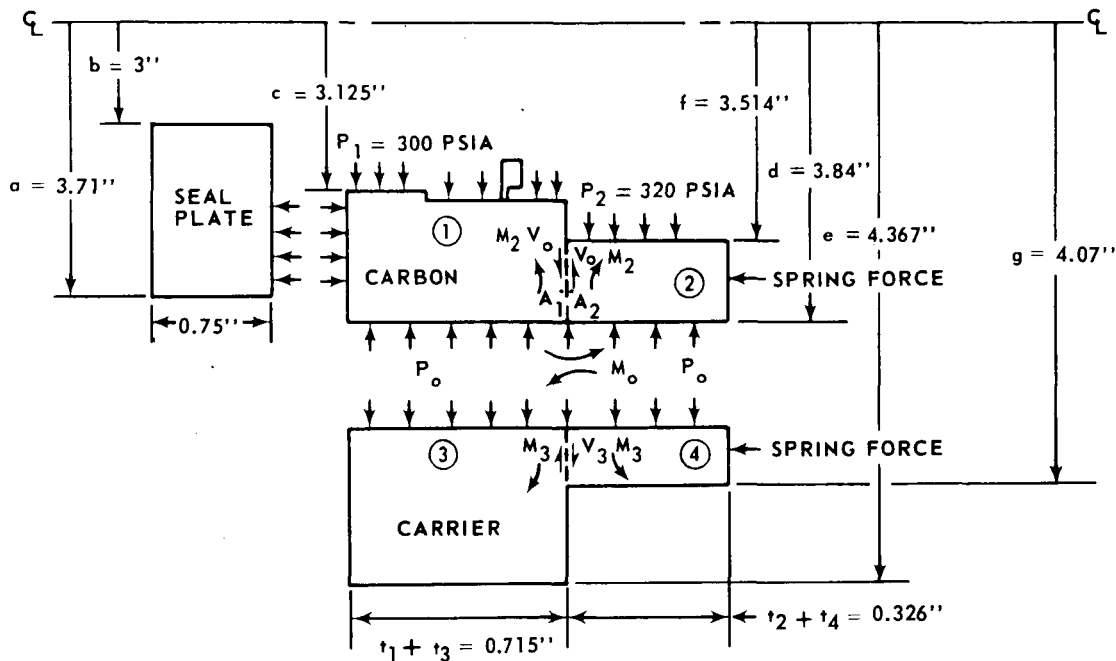
Figure 7   Dimensions and Loading for Externally Pressurized Hydrostatic Seal Analysis

For body number 1,

$$\delta_1 = \frac{P_1 d}{E_1}\left(\frac{2c^2}{d^2 - c^2}\right) - \frac{P_o d}{E_1}\left(\frac{c^2 + d^2}{d^2 - c^2} - v_1\right) - \frac{V_o}{2D_1 \lambda_1^3} + \frac{M_2}{2D_1 \lambda_1^2}$$

(10)

where:

P_1 = 300 psia

E_1 = 3 x 10^6 psi (Young's modulus of elasticity for carbon)

V_1 = 0.25 (Poisson's ratio)

c = 3.125 in

d = 3.84 in

V_o = transverse shear normal to wall

M_2 = uniform radial moment

$$D_1 = E_1 t^3 / 12 (1 - v_1^2) \tag{11}$$

t_1 = 0.715 in

$$\lambda_1 = \sqrt[4]{\frac{3(1 - v_1^2)}{R_{m_1}^2 t_1^2}} \tag{12}$$

R_{m_1} = 3.482 in.

For body number 2:

$$\delta_2 = \frac{P_2 d}{E_1} \frac{2f^2}{d^2 - f^2} - \frac{P_o d}{E_1} \left(\frac{f^2 + d^2}{d^2 - f^2} - v_1 \right) + \frac{V_o}{2D_2 \lambda_2^3} - \frac{M_2}{2D_2 \lambda_2^2} \tag{13}$$

where:

P_2 = 320 psia

f = 3.514 in.

d = 0.84

t = 0.326 in (for calculating D_2 and λ_2)

R_{m_2} = 3.677 in (for calculating λ_2)

For body number 3:

$$\delta_3 = \frac{P_o e}{E_2} \frac{2d^2}{e^2 - d^2} + \frac{V_3}{2D_3 \lambda_3^3} - \frac{M_3}{2D_3 \lambda_3^2} \tag{14}$$

where:

$$e \quad = \; 4.367 \text{ in}$$
$$t \quad = \; 0.715 \text{ in}$$
$$R_{m_3} \; = \; 4.103 \text{ in}$$

For body number 4:

$$\delta_4 \; = \; \frac{P_o g}{E_2} \quad \frac{2d^2}{g^2 - d^2} \quad - \quad \frac{V_3}{2D_4 \lambda_4^{\,3}} \quad + \quad \frac{M_3}{2D_4 \lambda_4^{\,2}} \tag{15}$$

where:

$$g \quad = \; 4.07 \text{ in}$$
$$E_2 \quad = \; 30 \times 10 \text{ psi (Young's modulus of elasticity for steel)}$$
$$t \quad = \; 0.326 \text{ in}$$
$$R_{m_4} \; = \; 3.96 \text{ in}$$

The equations for the angular displacement of each of the bodies are as follows.
For body number 1:

$$\theta_1 \; = \; - \, \frac{V_o}{2D_1 \lambda_1^{\,2}} \quad + \quad \frac{M_2}{\lambda_1 D_1} \quad + \quad \frac{M_o}{\lambda_1 D_1} \tag{16}$$

For body number 2:

$$\theta_2 \; = \; \frac{V_o}{2D_2 \lambda_2^{\,2}} \quad - \quad \frac{M_2}{\lambda_2 D_2} \quad + \quad \frac{M_o}{\lambda_2 D_2} \tag{17}$$

For body number 3:

$$\theta_3 \; = \; \frac{V_3}{2D_3 \lambda_3^{\,2}} \quad - \quad \frac{M_3}{\lambda_3 D_3} \quad - \quad \frac{M_o}{\lambda_3 D_3} \tag{18}$$

For body number 4:

$$\theta_4 \; = \; - \, \frac{V_3}{2D_4 \lambda_4^{\,2}} \quad + \quad \frac{M_3}{\lambda_4 D_4} \quad - \quad \frac{M_o}{\lambda_4 D_4} \tag{19}$$

Angular and radial displacements are equated to ensure continuity of structure:

$$\delta_1 = \delta_2 \qquad \theta_1 = \theta_2$$

$$\delta_3 = \delta_4 \qquad \theta_3 = \theta_4 \qquad (20)$$

$$\delta_1 = \delta_3 \qquad \theta_1 = \theta_3$$

These equations were solved simultaneously and the following results were obtained.

Pressure Associated with Press Fit, P_o	218. 78 psia
Radial Deflection, δ	0. 00028 in
Angular Deflection, θ	$-$ 0. 00002 in/in

c. CARBON FACE-CONTACT SEAL WITH BELLOWS SECONDARY SEAL

The analysis of the carbon face contact seal with a bellows secondary seal to determine deflections was also based on the equations of Roark. Seal plate deflections are the same as for the other Stein-designed seals.

The seal was assumed to be composed of the sections shown in Figure 8.
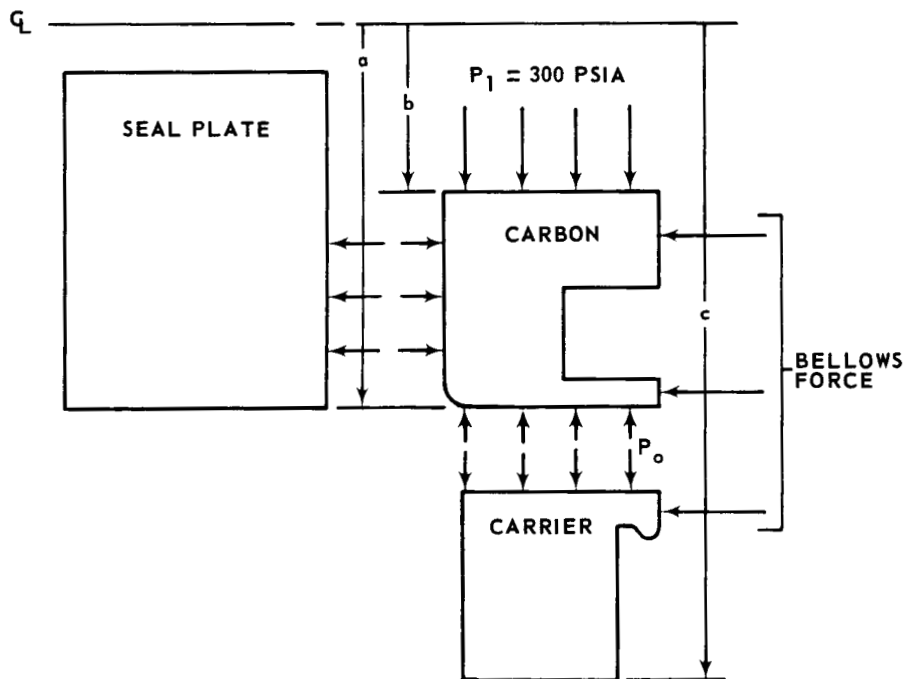
Figure 8   Analytical Sections of Carbon Face-Contact Seal With Bellows
Secondary Seal

The radial deflection of the carbon, δ_{carbon}, is represented by the equation,

$$\delta_{carbon} = \frac{P_1(a)}{E_1}\left(\frac{2b^2}{a^2 - b^2}\right) - \frac{P_0(a)}{E_1}\left(\frac{b^2 + a^2}{a^2 - b^2} - v_1\right) \qquad (21)$$

where:

P_0 = Pressure associated with the press fit between the carbon and the carrier

P_1 = 300 psia

E_1 = 3×10^6 (Young's modulus of elasticity for carbon)

v = 0.25 (Poisson's ratio)

a = 3.75 in

b = 3.1 in

The radial deflection of the carrier is represented by the equation,

$$\delta_{carrier} = \frac{P_0(a)}{E_2}\left(\frac{a^2 + c^2}{c^2 - a^2} + V_2\right) \qquad (22)$$

where:

E_2 = 30×10^6 (Young's modulus of elasticity for steel)

c = 4.1 in

The deflections of the carbon and the carrier are equal to ensure continuity of structure, and, therefore, P_0 can be determined thus:

$$P_0 = 208.35 \text{ psi} \qquad (23)$$

and

$$\delta_{carbon} = \delta_{carrier} = 0.00030 \text{ in} \qquad (24)$$

3. THERMAL ANALYSIS

a. CARBON FACE-CONTACT SEAL WITH PISTON RING SECONDARY SEAL

The results of the first thermal analysis for the carbon face-contact seal with piston ring secondary seal were presented in reports PWA-2837 and PWA-2879.

This analysis was modified to permit energy to bypass the oil passages in the seal plate. The resulting temperature distribution is shown in Figure 9. Figure 10 shows the temperature field for reduced rotational speed and Figure 11 shows the temperature field for no heat generation at the interface. A test was run at the conditions used for calculating data for Figure 10, and the measured temperatures were found to be between those presented in Figure 10 and those in Figure 11. Hence, it appears that the calculated power generation term based on the assumed coefficient of friction and loading force is too high. Two further modifications to the analysis are possible: a lower coefficient of friction could be assumed or it can be assumed that the seal was film-riding. The second of the assumptions was chosen and the analysis was performed as follows.

- Rubbing Contact Seal
    Coefficient of Friction 0.3
    Normal Load Force 17 lbs.
- Power Generation at Seal Interface: 200 Btu/Min (17,000 rpm) 500 fps.
- No Heat Removal by Leakage Air
- Heat Transfer Coefficient at:
    Stationary Surfaces: 1.0 Btu/Hr-Ft^2-°F
    Oil Passage in Seal Plate 865 Btu/Hr-Ft^2-°F
    Oil Passage in Bearing Race 260. Btu/Hr-Ft^2-°F
    Rotating Surfaces 200.-240. Btu/Hr-Ft^2-°F
- 15 Lbs/Min Oil Flow (100% Scoop Efficiency)
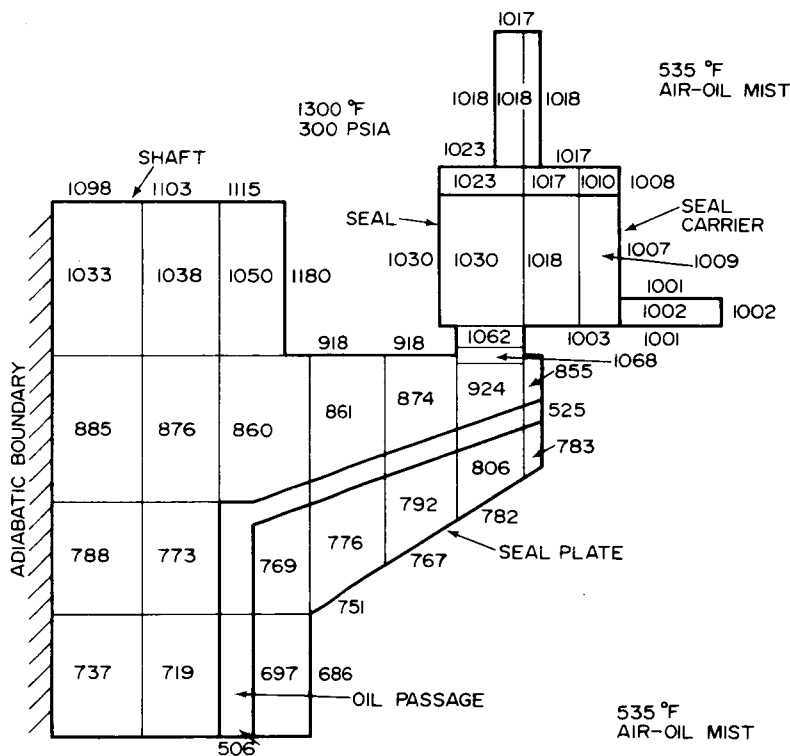
Figure 9   Calculated Temperature Field for Carbon Face-Contact Seal With Piston Ring Secondary Seal at Design Conditions

- Rubbing Contact Seal
    Coefficient of Friction 0.3
    Normal Load Force 17 lbs.
- Power Generation at Seal Interface: 160 Btu/Min (13,640 rpm) 400 fps.
- No Heat Removal by Leakage Air
- Heat Transfer Coefficient at:
    Stationary Surfaces 1.0 Btu/Hr-Ft^2-°F
    Oil Passage Seal Plate 865 Btu/Hr-Ft^2-°F
    Oil Passage in Bearing Race 260. Btu/Hr-Ft^2-°F
    Rotating Surfaces 100. Btu/Hr-Ft^2-°F
- 15 Lbs/Min Oil Flow (100% Scoop Efficiency)

Figure 10   Calculated Temperature Field for Carbon Face-Contact Seal With
Piston Ring Secondary Seal at Reduced Rotational Speed

- Zero Power Generation at Interface
- No Heat Removal by Leakage Air
- Heat Transfer Coefficient at:
    - Stationary Surfaces 1.0 Btu/Hr-Ft^2-°F
    - Oil Passage in Seal Plate 865. Btu/Hr-Ft^2-°F
    - Oil Passage in Bearing Race 260 Btu/Hr-Ft^2-°F
    - Rotating Surfaces 100. Btu/Hr-Ft^2-°F
- 15 Lbs/Min Oil Flow (100% Scoop Efficiency)
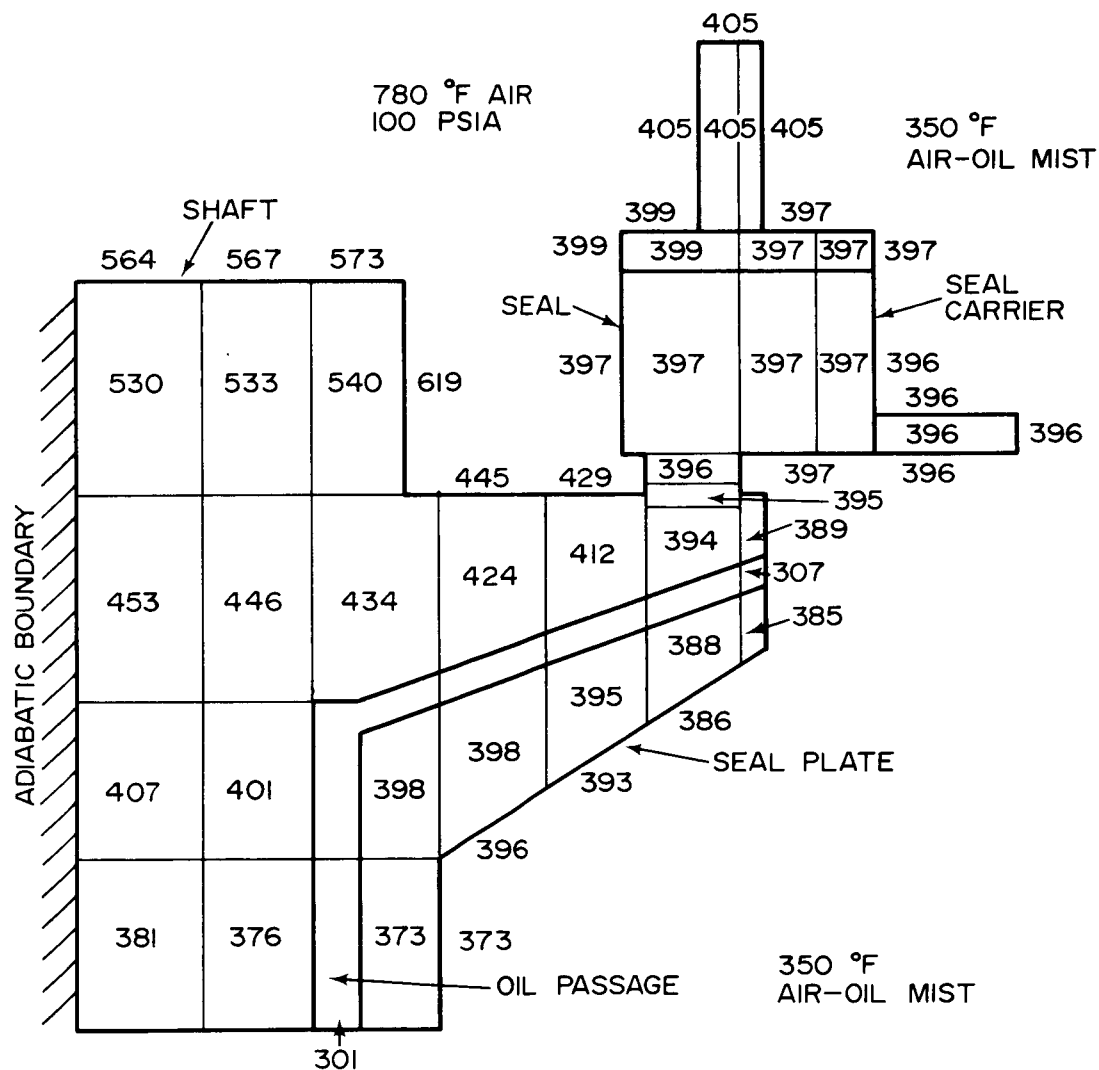
Figure 11   Calculated Temperature Field for Carbon Face-Contact Seal With
Piston Ring Secondary Seal and No Heat Generation at Interface

Consider a control element (Figure 12) into which a fluid enters with enthalpy rate WC_pT_O and out of which a fluid leaves with enthalpy rate $WC_p\left[T_O+(dT_O/dx)dx\right]$ Total power generation within the element is defined as $PLdx$.
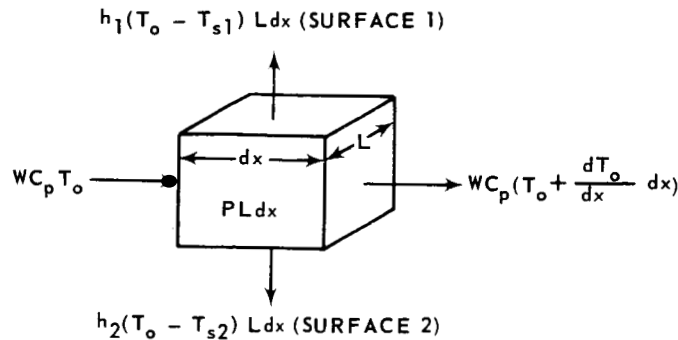
Figure 12   Analytical Element for Seal Temperature Field Calculation Based On Film-Riding Assumption

The heat transfer rates from the element to surfaces 1 and 2 are $h_1(T_O-T_{s1})Ldx$ and $h_2(T_O-T_{s2})Ldx$, respectively.

At steady-state conditions, the rates that energy enters and leaves the element are equal. Therefore,

$$WC_p\,T_O+PLdx = WC_p(T_O+\frac{dT_O}{dx}\,dx) + h_1(T_O-T_{s1})Ldx + h_2(T_O-T_{s2})Ldx \qquad (25)$$

Rearranging,

$$\frac{dT_O}{dx} + (h_1 + h_2)\ \frac{L}{WC_p}T_O\ -(h_1T_{s1} + h_2\,T_{s2})\frac{L}{WCP}\ -\ \frac{PL}{WC_p} = 0 \qquad (26)$$

where:

W	=	Mass fluid flow (lb/hr)
C_p	=	Specific heat at constant pressure of fluid (Btu/lb-°F)
T_O	=	Temperature of fluid (function of x), (°F)
h_1, h_2	=	Heat transfer coefficients at surfaces 1 and 2 respectively, Btu/hr-ft^2-°F)
Ldx	=	Surface area on either side of fluid (Ft^2)
P	=	Uniform power generation per surface (Btu/hr-ft^2)
$T_{s1},\ T_{s2}$ =		Temperature of surfaces 1 and 2 respectively, (°F) (assumed to be constant within the element dx)
x	=	coordinate in direction of fluid flow (ft)

By defining:

$$K = \frac{L}{WC_p} (h_1 T_{s1} + h_2 T_{s2} + P) \tag{27}$$

and substititing into equation 26,

$$\frac{dT_o}{dx} + (h_1 + h_2) \frac{L}{WC_p} T_o - K = 0 \tag{28}$$

Rearranging:

$$\frac{\dfrac{dT_o}{KWC_p}}{T_o - \dfrac{KWC_p}{(h_1 + h_2)L}} + \frac{(h_1 + h_2) L dx}{WC_p} = 0 \tag{29}$$

Equation 29 can be integrated directly if everywhere within the limits of integration the denominator of the first term does not equal zero.

Also, to justify the assumption that T_{s1} and T_{s2} are constants within dx, the range of integration should be small. In terms of applying the solution of equation 29 to a finite-difference program on a digital computer, the assumption presents no obstacle because temperatures must be taken as constant for finite distances. Integrating equation 29 for

$$0 \le x \le W \tag{30}$$
$$T_{o1} \le T_o \le T_{o2}$$

Yields:

$$\ln \left[\frac{T_{o2} - \dfrac{KWC_p}{(h_1 + h_2)L}}{T_{o1} - \dfrac{KWC_p}{(h_1 + h_2)L}} \right] + \frac{(h_1 + h_2)Lw}{WC_p} = 0 \tag{31}$$

Defining:

$$\frac{h_1 L_w}{WC_p} \equiv NTU_1 \quad \text{and} \quad \frac{h_2 L_w}{WC_p} \equiv NTU_2 \tag{32}$$

Substituting equations 32 into 31 and rearranging yields:

$$T_{o1} - \frac{KWC_p}{(h_1+h_2)L} = \left(e^{NTU_1 + NTU_2}\right)\left(T_{o2} - \frac{KWC_p}{(h_1+h_2)L}\right) \tag{33}$$

Equation 33 is the solution to the differential equation 26 but its form can not be used in the TOSS computer program. The following analysis was, therefore, required to alter equation 33 to a form suitable for the TOSS program.

To simplify the algebraic manipulations, equation 33 was written in the form

$$T_{o1} - Y = Z (T_{o2} - Y) \tag{34}$$

where:

$$Y = \frac{KWC_p}{(h_1+h_2)L} \tag{35}$$

$$Z = e^{NTU_1 + NTU_2} \tag{36}$$

Multiplying both sides of equation 34 by WC_p and rearranging yields:

$$YWC_p (Z-1) = WC_p (ZT_{o2} - T_{o1}) \tag{37}$$

Adding and substracting $WC_p T_{o2}$ to the right-side of equation 37 and rearranging yields:

$$WC_p(T_{o2} - T_{o1}) = WC_p(Z-1) (Y-T_{o2}) \tag{38}$$

The left side of equation 38 is recognizable as the rate of change of fluid enthalpy. To facilitate the identification of the right side of equation 38, the parameter Y is written in terms of its constituents. Equation 38 becomes

$$WC_p(T_{o2} - T_{o1}) = WC_p(Z-1)\left(\frac{h_1 T_{s1} + h_2 T_{s2} + P}{h_1 + h_2} - T_{o2}\right) \tag{39}$$

or,

$$WC_p(T_{o2} - T_{o1}) = WC_p \frac{(Z-1)P}{h_1+h_2} + WC_p(Z-1)\left(\frac{h_1}{h_1+h_2}(T_{s1}-T_{o2}) + \frac{h_2}{h_1+h_2}(T_{s2}-T_{o2})\right) \tag{40}$$

Multiplying the numerator and denominator of the right side of equation (40) by the surface area, L_w, and substituting equation 32 into the result yields

$$WC_p(T_{o2}-T_{o1}) = \frac{Q(Z-1)}{NTU_1 + NTU_2} + \frac{(Z-1)}{NTU_1+NTU_2}\left(h_1 A(T_{s1} - T_{o2}) + h_2 A(T_{s2} - T_{o2})\right) \tag{41}$$

where:

$$Z = e^{NTU1 + NTU2}$$
$$Q = PL_w = \text{Total power generation in the fluid (Btu/hr)}$$
$$A = L_w = \text{Area of either surface (ft}^2)$$

Finally, equation 41 may be written as

$$WC_p(T_{o2} - T_{o1}) = Q + Q\left(\frac{Z-1-NTU_1-NTU_2}{NTU_1+NTU_2}\right)$$
$$+ \frac{(Z-1)A}{NTU_1+NTU_2}\left(h_1(T_{s1} - T_{o2}) + h_2(T_{s2} - T_{o2})\right) \tag{42}$$

The sum of the second and third terms on the right side of equation 42 is seen to be the effective convection heat transfer between the surfaces and the fluid. The sum of the first and second terms is the effective power generated within the fluid. The following electrical analogue sketch shown in Figure 13 demonstrates the internal connections made in the TOSS program.

$$H_{E_1} = \frac{h_1(Z-1)}{NTU_1 + NTU_2}$$

$$H_{E_2} = \frac{h_2(Z-1)}{NTU_1 + NTU_2}$$

$$Q_E = \frac{Q(Z-1)}{NTU_1 + NTU_2}$$
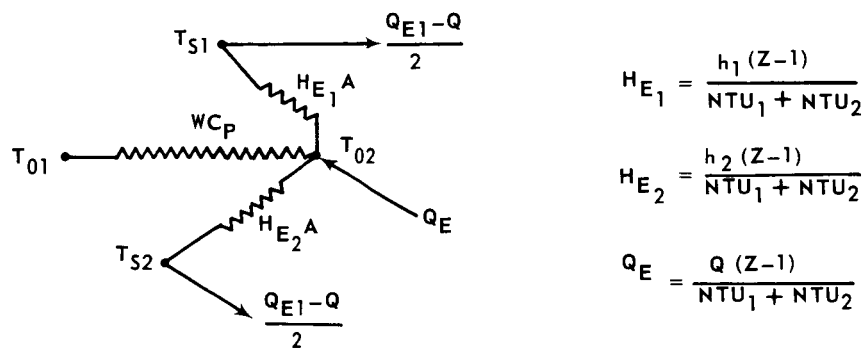
Figure 13   Electrical Analog of Seal Heat Transfer Analysis

The conductance connection between fluid nodes is WC_p. The conductance connection between the surface and fluid nodes is $H_E A$. An amount of power equal to $1/2 \ (Q_E - Q)$ is removed from each surface via a "dummy" boundary node. An amount of power equal to Q_E is added to the downstream fluid node via another "dummy" boundary node. Note that the net influx of power to the system is equal to Q.

The power generated within the fluid is calculated from

$$Q = \frac{4 \pi^2 \mu A N^2 r^2}{g_c J S} \tag{43}$$

where,

Q = Heat generated (Btu/hr)
μ = Viscosity of the fluid (lb mass/ ft sec)
g_c = Gravitational constant
A = Area of rubbing surface (ft^2)
N = Rotational speed of seal plate relative to seal (rpm)
J = Mechanical equivalent of heat (778 ft lb/Btu)
r = Mean radius of revolution (ft)
s = Separation distance (thickness of fluid) between seal and seal plate (ft)

The heat transfer surface coefficients are determined from forced convection considerations. The Reynolds modulus of the fluid is:

$$Re = \frac{DW}{\mu A_{flow}} \tag{44}$$

where:

A_{flow} = Flow area (ft^2)

The characteristics flow dimension used is the hydraulic diameter, D. At any radius, r:

$$D = \frac{4 A_{flow}}{P_w} = \frac{4 (2 \pi r \ S)}{2 (2 \pi r)} = 2S \tag{45}$$

where:

P_w = Wetted perimeter of the flow passage (ft)

Consequently, at any radius

$$Re = \frac{W}{\pi r \mu} \tag{46}$$

Finally, h_1 and h_2 are determined from the approximate Nusselt modulus:

$$Nu = \frac{hD}{K} = \frac{2hS}{K} \tag{47}$$

where:

K = Thermal conductivity of the fluid (Btu/hr-ft-°F)

The relationship between equations 46 and 47 depends, of course, on whether the flow is laminar, transitional, or turbulent.

Temperature values calculated on the basis of this analysis will be compared with the experimentally determined temperatures to determine if the film-riding model is more accurate than the rubbing-contact model.

b. ORIFICE-COMPENSATED HYDROSTATIC FACE SEAL

The film portion of the orifice-compensated hydrostatic face seal will be analyzed using equation 42.

B.   TASK II - MAIN-SHAFT SEAL EVALUATION

1.   INTRODUCTION

Task II has three objectives: the procurement of four seal assemblies of each of the four seal designs after the designs are approved by the NASA project manager, the design and procurement of test equipment capable of testing the seals at the design conditions, and an experimental evaluation program for each seal design.

2.   SEAL PROCUREMENT

NASA approval of the externally pressurized hydrostatic seal was obtained during the report period. Approval of the other three seal designs had been received previously.

Detail drawings of the face contact seal with piston ring secondary seal were included in the first semiannual progress report (PWA-2863). Detail drawings of the face contact seal with bellows secondary seal and of the orifice compensated hydrostatic face seal were included in the second semiannual progress report (PWA-2879). Detail drawings of the externally pressurized hydrostatic face seal are included in the appendix of this report.

The first externally pressurized hydrostatic face seal was received on December 27, 1966, and is shown in Figures 14 through 19.

All seals are now available except the face-contact seal with bellows secondary seal, which is expected on January 30, 1967.
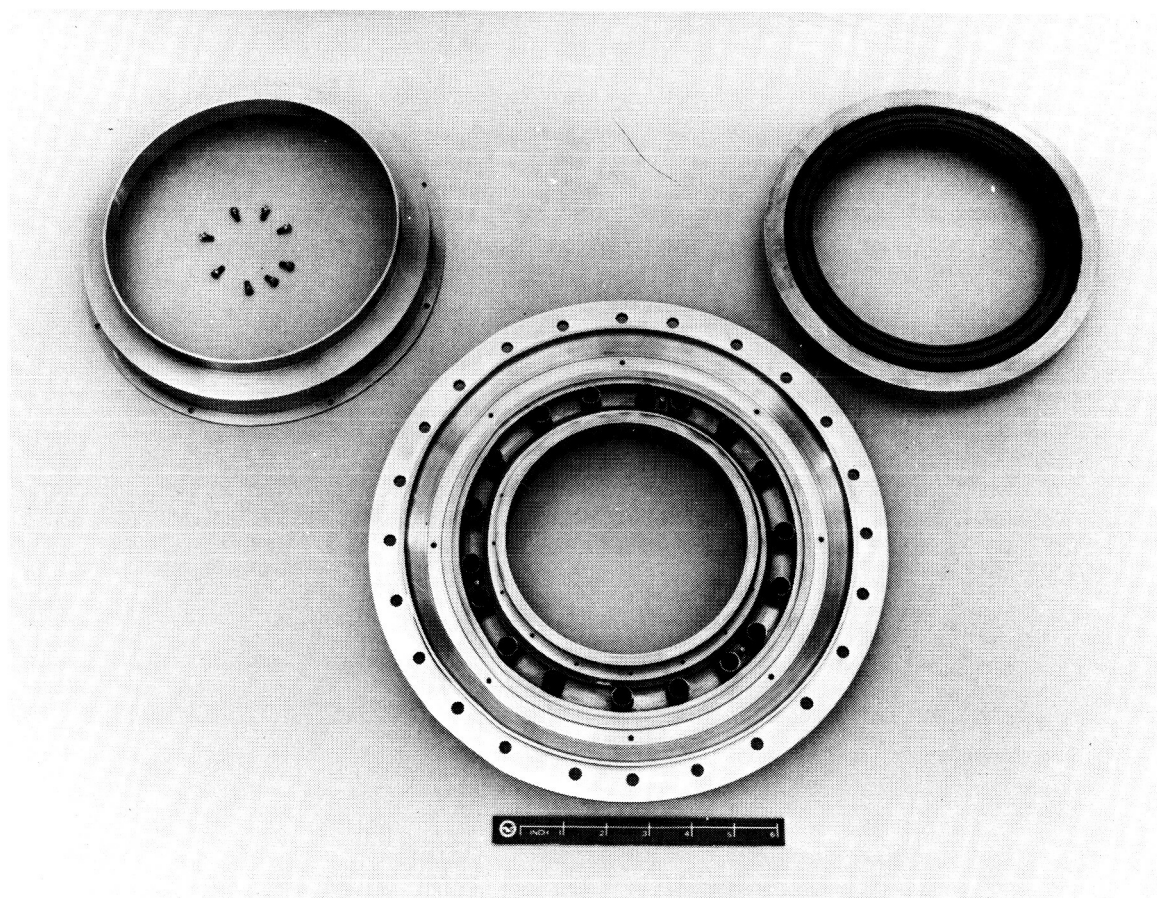
Figure 14   Component Parts of Externally Pressurized Orifice-Compensated
Hydrostatic Face Seal Assembly   CN-7466
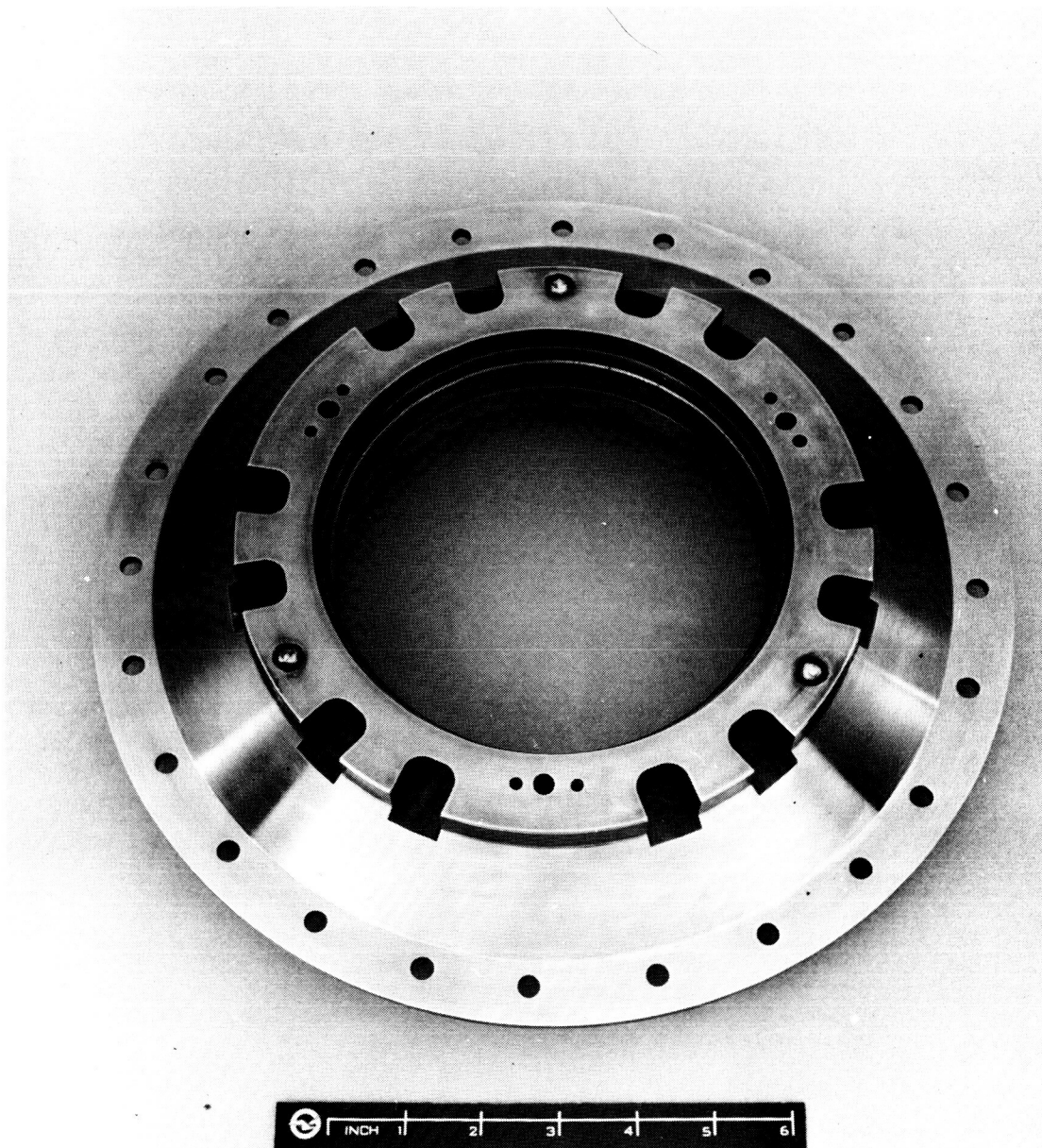
Figure 15   Seal Carrier from Externally Pressurized Orifice-Compensated
            Hydrostatic Face Seal Showing the Three Inlet Holes for
            Pressurizing Air Supply   CN-7467
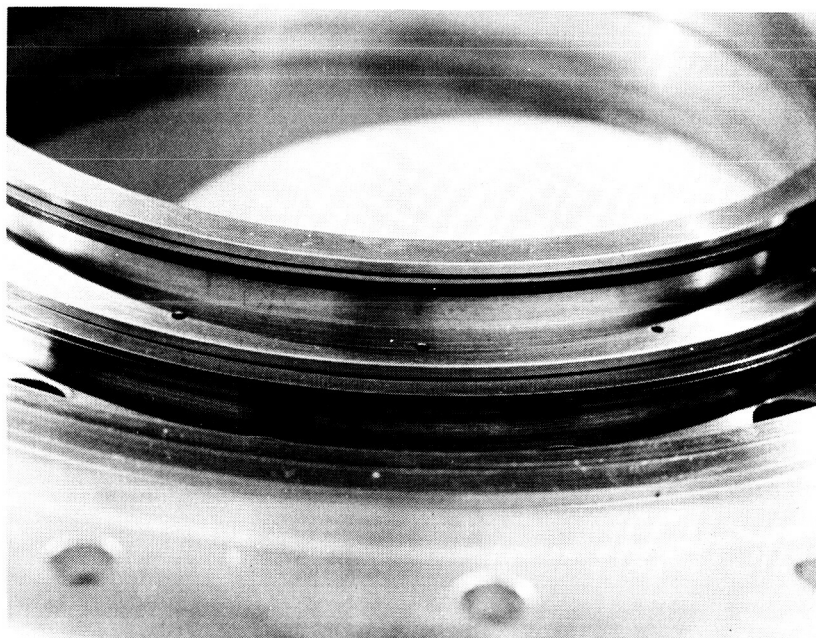
Figure 16   Close-up View of the High-Pressure Compartment of the Externally
            Pressurized Orifice-Compensated Hydrostatic Face Seal

CN-7471

Figure 17   Close-up View of Carbon Seal Ring Assembly of the Externally
            Pressurized Orifice-Compensated Hydrostatic Face Seal Showing
            One of the Four Annular Segments With Orifice and Bleed Hole
            Annulus   CN-7469

Figure 18   Close-up View of Rear of Carbon Seal Ring Assembly of the Ex-
ternally Pressurized Orifice-Compensated Hydrostatic Face Seal
Showing an Orifice, Bleed Holes Without Orifice, and Anti-Torque
Pin Hole   CN-7470
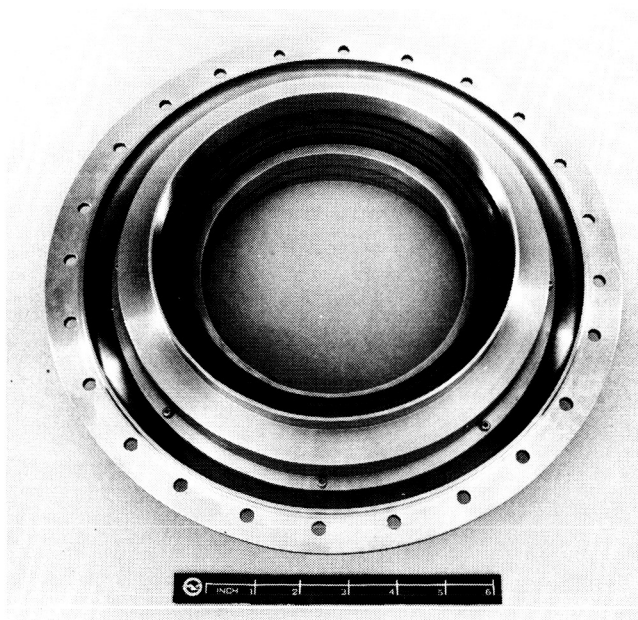
Figure 19   Externally Pressurized Orifice-Compensated Hydrostatic Face Seal
Assembly   CN-7468

3. TEST FACILITIES

The seal tests are being run in two test stands, each of which is completely enclosed with the control panel and instrumentation located outside the test area. The rigs are bed-plate mounted and driven by Ford industrial engines through five-speed truck transmissions and 12 to 1 ratio gearboxes. Facilities for heating the oil required for the test are located in the test cell, and the heated air is piped from electrical air heaters. A schematic diagram of the test facilities is shown in Figure 20. Views of the test stands are shown in Figures 21 through 24. A general view of the mechanical components test area is shown in Figure 25, and the control panel for X-119 stand is shown in Figure 26. The seal test rigs were designed to permit all seals to be tested without the use of special adapters. All seals were designed with the same bolt circle and axial length.
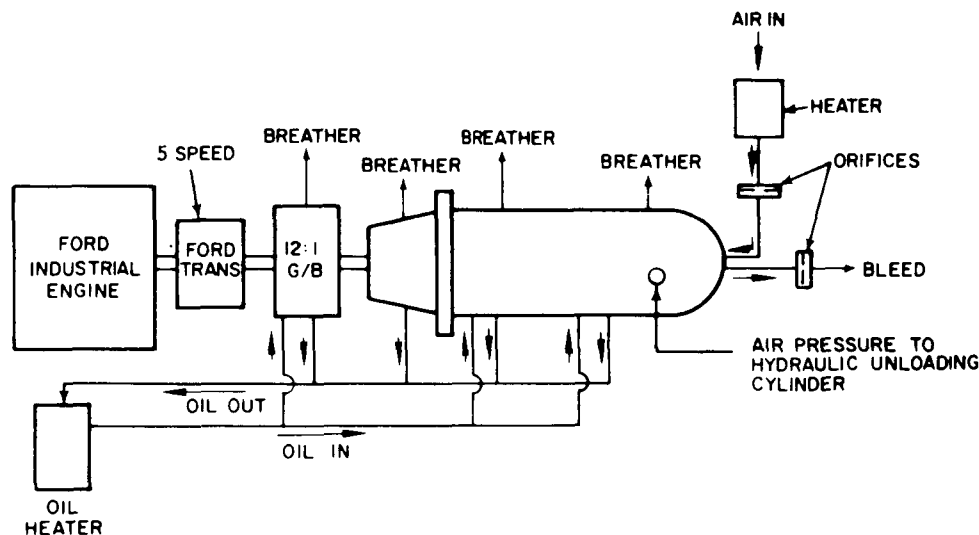
Figure 20   Schematic Diagram of Seal Test Facility

The inert gas test rig will be a modification of one of the seal test rigs and will be used to test the three best seals in a nitrogen atmosphere. The modifications required are shown in Figure 27. All of the parts required for the modification have been procured. The rig will be assembled after the endurance test phase of the program has been completed.

A current seal test rig was modified to develop the instrumentation techniques necessary to measure seal-face-generated torque and seal axial forces. All parts were procured during the previous six-month period, and testing was started early in the current report period. A schematic diagram of the instrumentation validation rig is shown in Figure 28.
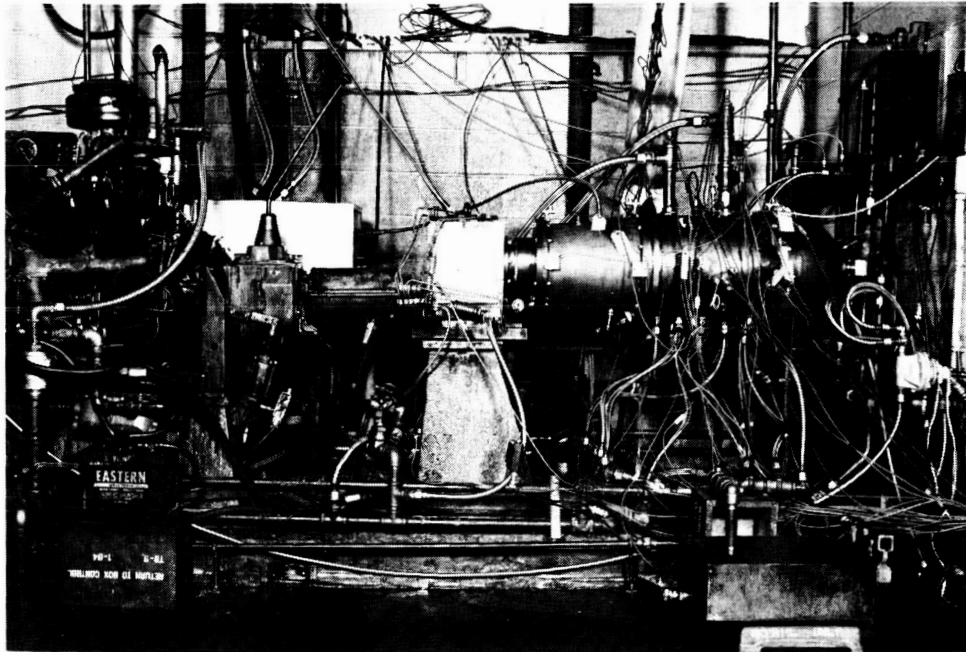
Figure 21   Over-all View of X-81 Stand Showing Test Rig, Gear Box, and
            Drive Engine   CN-5980
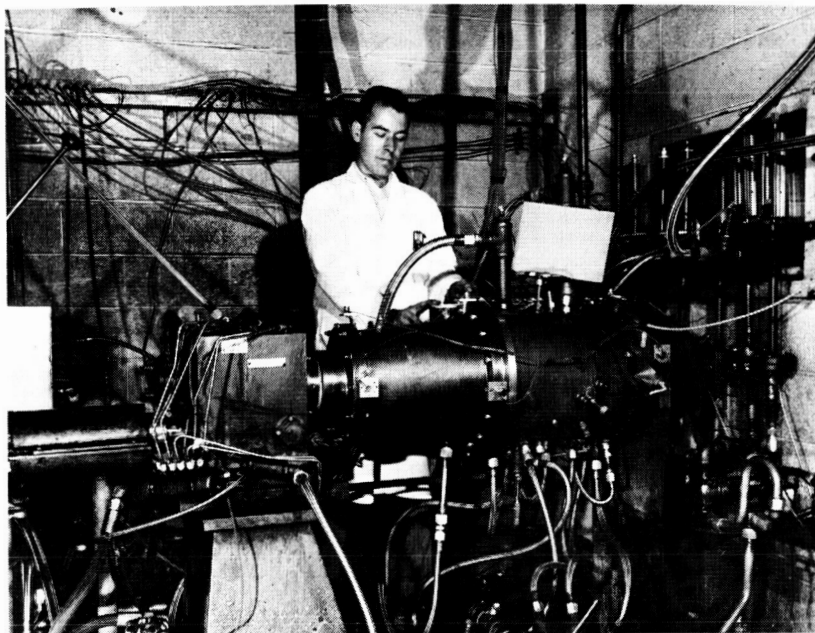
Figure 22   Installation of Main-Shaft Seal Rig in X-81 Stand   CN-7081
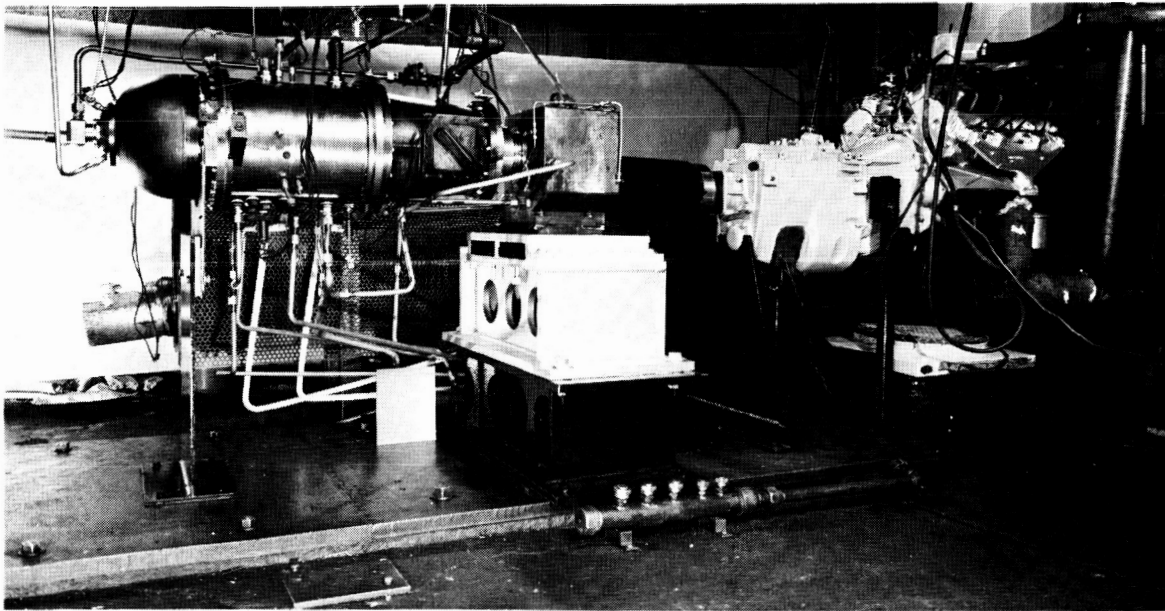
Figure 23   Over-all View of X-119 Stand Showing Main-Shaft Seal Rig B,
Gearbox, and Drive Engine   CN-6928
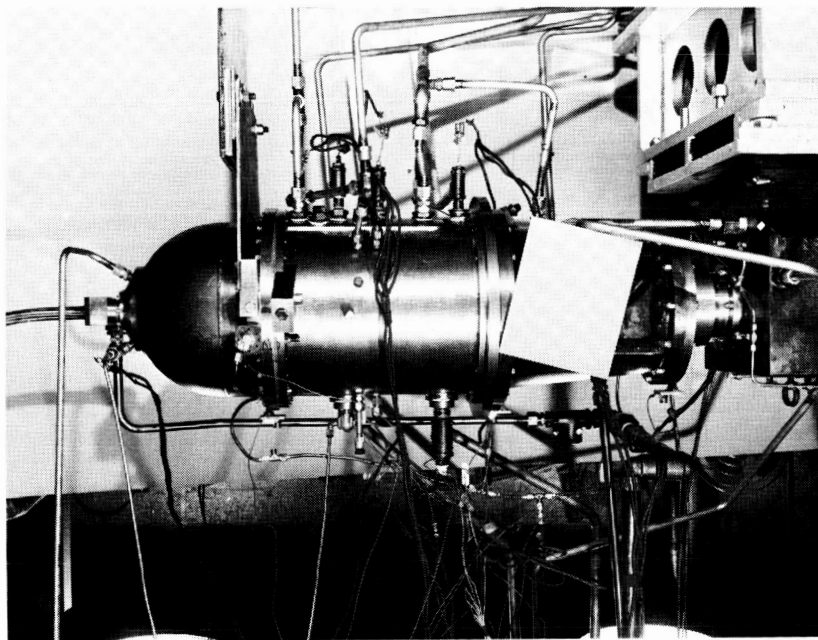
Figure 24   Close-up View of Seal Rig B in X-119 Stand   CN-6929
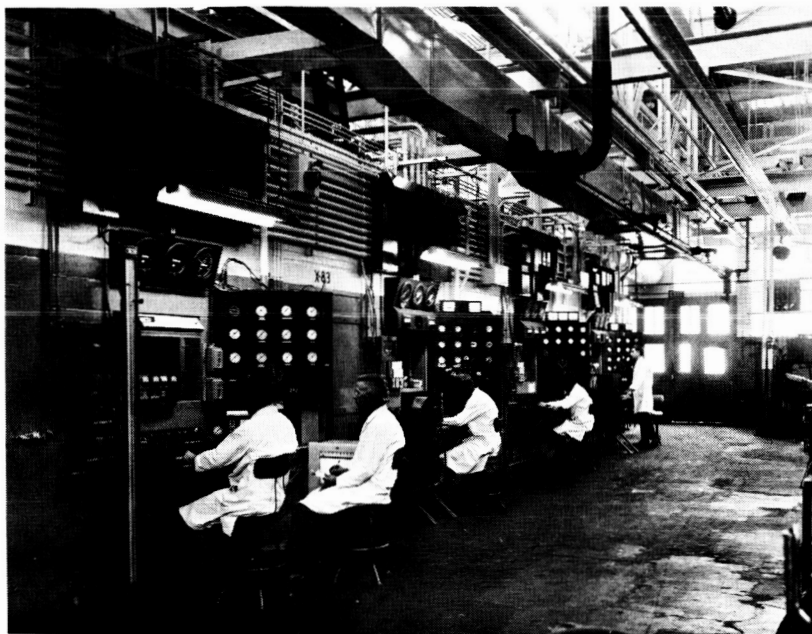
Figure 25   Mechanical-Components Test Area Where Main-Shaft Seal Rig Test
Program is being Conducted   CN-7079

Figure 26   Control Panel for X-119 Test Stand   CN-6930

INSULATION
REMOVED

ORIGINAL DOME
COVER

DOME MOVED
TO ACCEPT ADDED
PARTS

ORIGINAL
DOME COVER

LONGER BOLT
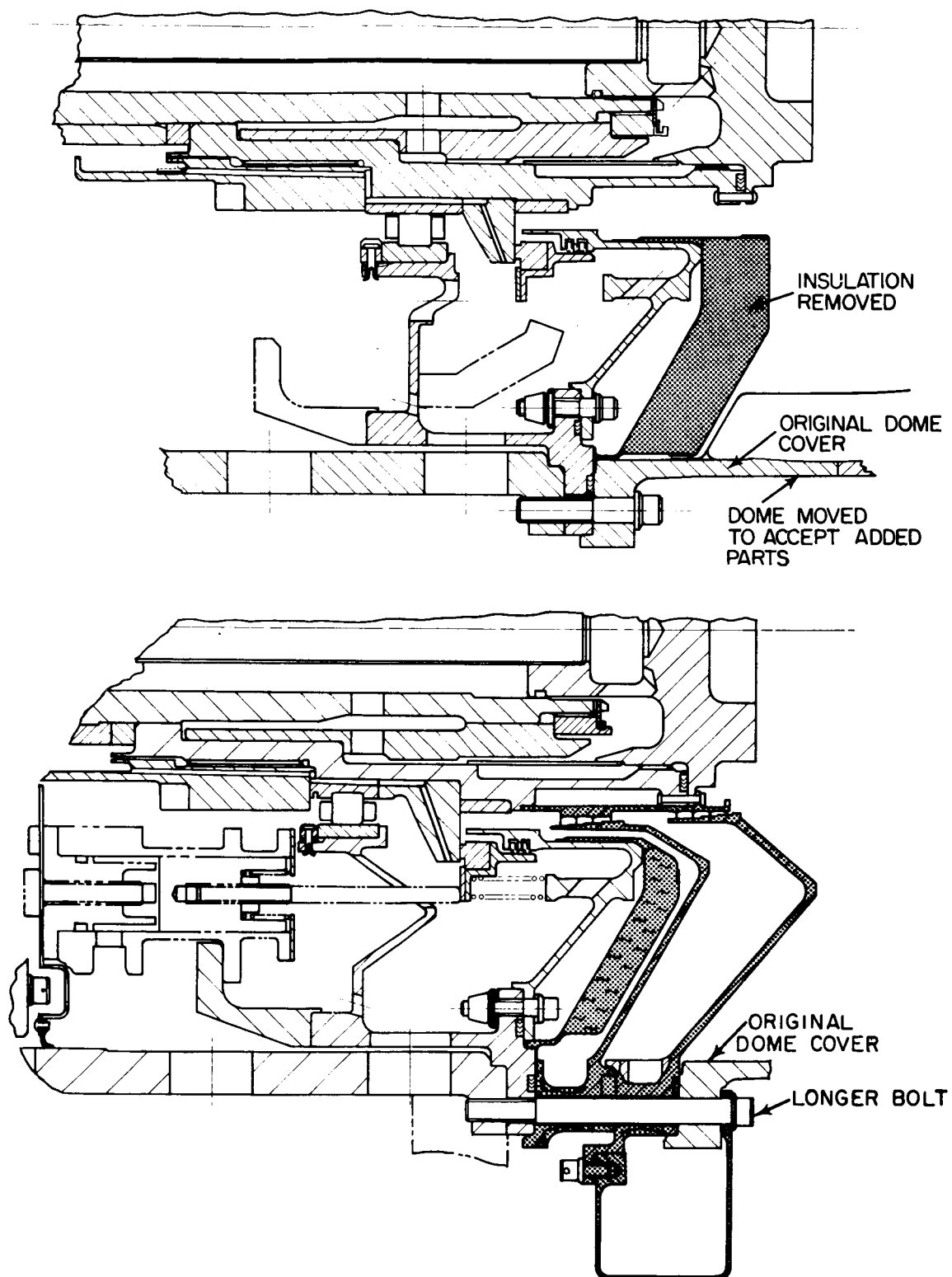
Figure 27   Modifications Required to Seal Test Rig for Inert Gas Testing.
Changes are Shown by Shading.

1 SEAL PLATE
2 ACCELEROMETER
3 SEAL ASSEMBLY
4 PISTON ROD
5 CYLINDER AND PISTON
  ASSEMBLY
6 PROXIMITY PICKUP
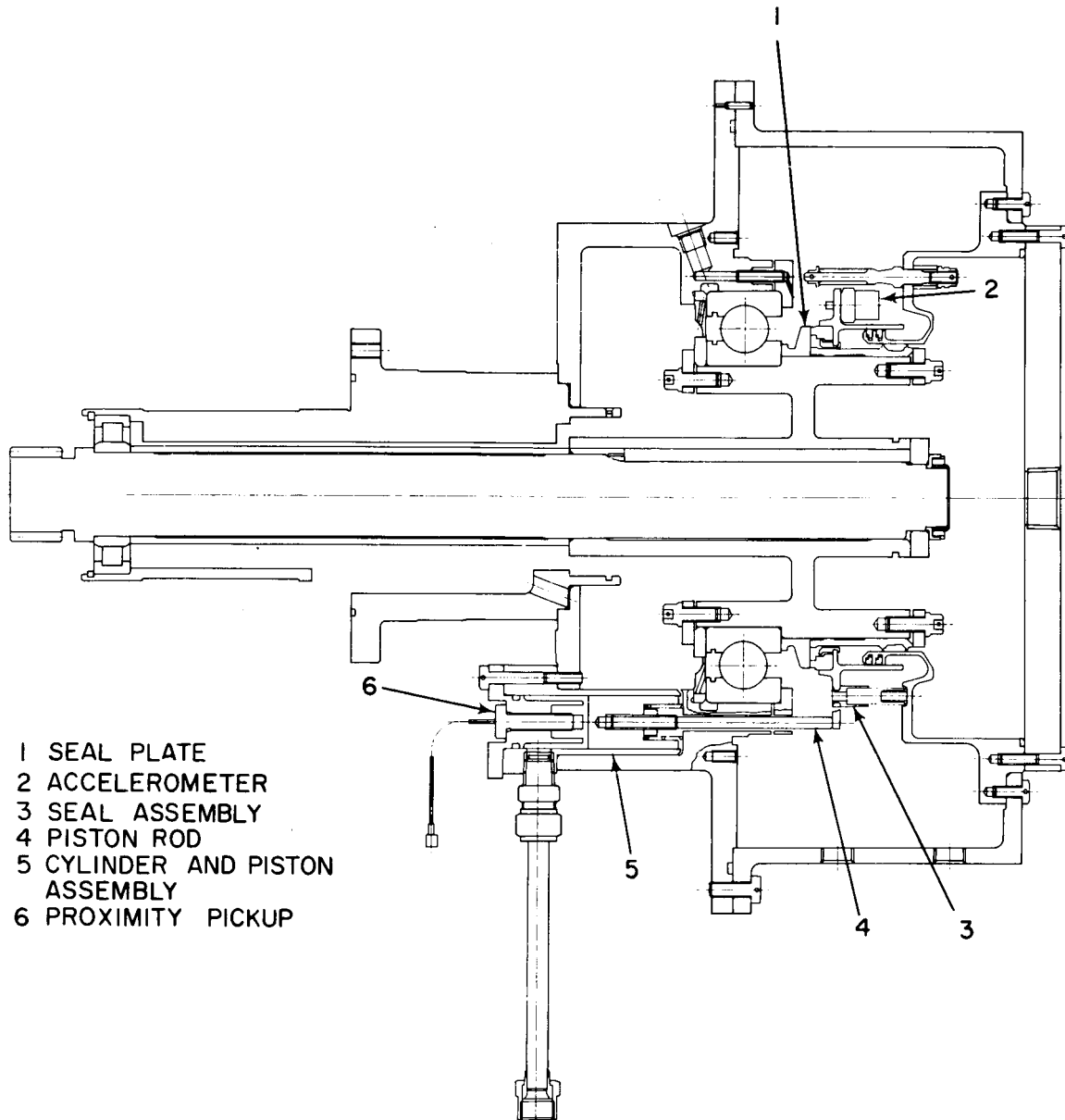
Figure 28   Instrumentation Validation Rig

4. EXPERIMENTAL PROGRAM

a. RUBBING CONTACT FACE SEAL WITH PISTON RING SECONDARY SEAL

Six builds of the rubbing contact face seal with piston ring secondary seal have been tested.

Builds 1 and 2 - The results of the first build and of the dynamic tests of the second build were presented in the second semiannual report (PWA-2879) and are summarized in Table II together with the results from the other tests conducted during the period. These tests were run at various rubbing speeds using ambient air temperature and oil at 250°F. Table III presents the results of the pretest and post-test inspection data.

Simulated engine operation tests were run on Build 2 using oil at 250°F and gas at 800°F. The tests were performed at static conditions and at surface speeds of 200 and 300 ft/sec. The effect of temperature on leakage at a rubbing speed of 300 ft/sec is shown in Figure 29. As shown, the effect is negligible. The effect of speed on leakage is shown in Figure 30. The effect is negligible for
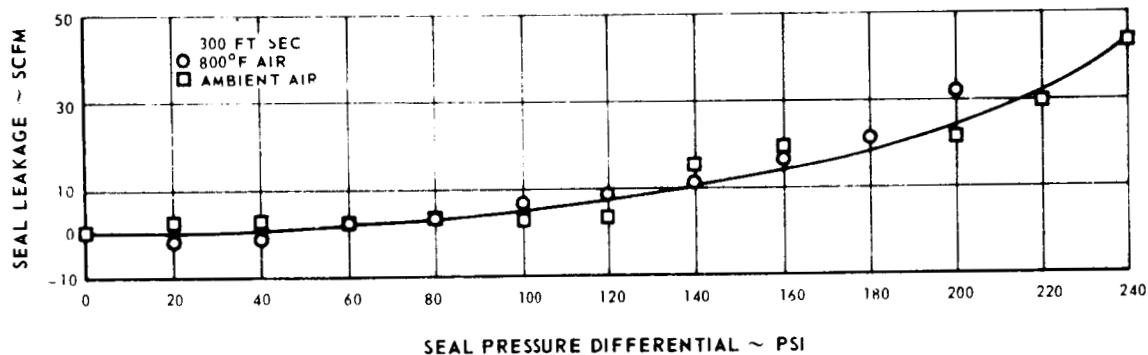
Figure 29   Effect of Temperature on Seal Leakage of Carbon Face Seal With Piston Ring Secondary Seal (Build 2)
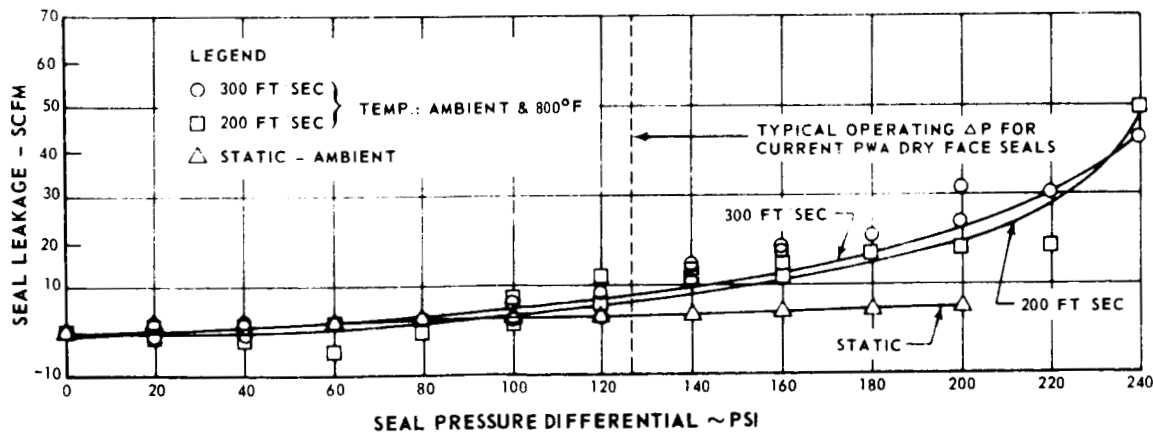
Figure 30   Effect of Surface Speed on Seal Leakage of Carbon Face Seal With Piston Ring Secondary Seal (Build 2)

FACE CONTACT SEAL WITH I

Build No.	Seal Plate	Carbon Seal	Other Special Features	PCO	SEO	20 Hr. Eng
1	New	New - wide carbon lip.	19.5 lb. Spring Load	X		
2	New	Carrier from Bld 1 with new carbon 0.150 in. lip.	Enlarged inlets to seal plate oil holes	X	X	
3	Relapped plate from Bld 1 with enlarged holes	New - incorrect seal lip width.	Oil jet manifold in seal area		X	
4	Used plate from Bld 3	Used - from Bld 3 reworked to correct lip width - relapped			X	
5	Relapped plate from Bld 4	Used - from Bld 4	Increased oil flow to roller brg & seal plate oil scoop. Additional jet to roller brg.		X	
6	Used plate from Bld 5	New			X	

Note: Unless stated otherwise, all carbon lips are 0.155 in. wide, all springs 30 lb. load.

PCO = Preliminary Check Out

SEO = Simulated Engine Operation

A

327

TABLE II

PISTON RING SECONDARY SEAL TEST SUMMARY

| – Tests – | | | | Reason for | Condition After Test | | Test |
No.	Cyc. End.	Max. Cap.	Inert Gas	Test Termination	Seal Plate	Carbon Seal	Hours
				Excessive air leakage – amb. air temp.		0.0002 in wear	16.00
				Excessive air leakage – amb. air temp.	Excessive wear	Excessive wear 0.0256 in wear	50.00
				Excessive air leakage – 800F air		0.0060 in. wear	5.75
				Excessive air leakage – 800 & 1000F air temp.	Very sl. wear	0.0020 in. wear	9.75
				Excessive air leakage – 800 & 1000F air temp.	O.K.	Carbon deposits on seal. 0.0025 in. wear	14.75
				Completed limited running of SEO with 250°F oil	Polished – Small am't. carbon varnish – slight depression in wear track.	0.0022 in. wear good condition	101.75

B

FACE CONTACT SEAL WITH
POST-TEST PERFO

Build No.		1	1	2
Test Condition		Pre	Post	Pre
	Units			
Static Seal Leakage				
At assembly - 80 psig	SCFM	0.13	0.56	0.05
At test stand - 20 psig	SCFM	≤1.2	≤1.2	≤1.2
40	SCFM	≤1.5	≤1.5	≤1.5
60	SCFM	≤1.8	1.9	≤1.8
80	SCFM	≤1.9	3.0	≤1.9
100	SCFM	≤2.2	3.6	2.4
120	SCFM	2.7	3.9	3.1
140	SCFM	3.4	3.4	3.6
160	SCFM	4.1	3.8	4.0
180	SCFM	4.9	4.6	4.5
200	SCFM	5.4	6.1	5.1
220	SCFM	5.6	7.5	5.7
240	SCFM	5.7	9.0	6.3
260	SCFM	7.0	10.2	6.6
Spring Rate in Assembly	lb/in.	52.3*	34.7*	30.0*
Total Spring Force (no piston rings)				
Tare wt (seal face assy)	lb	1.85	1.77	1.74
Total Load (normal assembled length)	lb	13.35	13.95	26.33
Total Load (operating length)	lb	19.60	18.20	32.2
Total Load (fully compressed)	lb	29.50	24.50	36.49
Hydraulic Loading from Seal Unbalance of Test Stand with Springs and Piston Rings Installed				
20 psig	lb	36.6*	8.9*	**
40	lb	38.1*	30.9*	**
60	lb	47.0*	36.0*	**
80	lb	59.0*	47.0*	**
100	lb	69.5*	75.5*	**
120	lb	90.3*	61.1*	**
140	lb	87.4*	81.1*	**
160	lb	93.6*	79.0*	**
180	lb	116.5*	51.0*	**
200	lb	123.2*	64.8*	**
220	lb	121.8*	82.7*	**
240	lb	128.5*	72.6*	**
260	lb	138.0*	82.7*	**
Carbon Dam Height				
0°	in.	0.1014	0.1014	0.0953
90°	in.	0.1011	0.1009	0.0953
Avg		0.1013	0.1011	0.0954
Flatness				
Seal plate	He lt. bands	≤2	9	1
Carbon	He lt. bands	1	9	3
Remarks		(19 lb spring load)		(32 lb spr

*Questionable data
**Data not taken - await validation rig study

A

33-1

TABLE III

PISTON RING SECONDARY SEAL PRETEST AND
RMANCE AND INSPECTION SUMMARY

2 Post	3 Pre	3 Post	4 Pre	4 Post	5 Pre	5 Post	6 Pre	6 Post
-	1.2	≥ 4.0	1.6	≥ 4.0	1.6	5.8	1.1	2.9
Excessive	≤1.2	-	≤1.2	26.6	≤1.2	11.5	≤1.2	Data
Excessive	1.6	27.3	1.5	45.8	1.3	21.2	≤1.5	Not
Excessive	1.9	48.6	2.4	68.1	1.9	27.5	≤1.8	Taken
Excessive	3.3	70.0	3.6	85.4	2.6	33.7	2.3	
Excessive	11.2	94.6	4.8	107.5	3.4	41.1	2.9	
Excessive	24.8	≥132.0	6.2	130.8	3.9	46.6	4.3	
Excessive	39.4	≥132.0	7.9	≥153.5	4.9	51.0	4.1	
Excessive	55.5	≥132.0	9.2	≥153.5	5.3	58.9	6.7	
Excessive	70.7	≥132.0	11.7	≥153.5	6.0	67.2	11.8	
Excessive	94.3	≥132.0	12.9	≥153.5	6.8	72.9	14.3	
Excessive	-	-	-	-	-	-	-	-
Excessive	-	-	-	-	-	-	-	-
Excessive	-	-	-	-	-	-	-	-
50.7	52.3	51.6	53.8	53.5	55.0	50.9	47.9	47.9
1.73	1.7	1.7	1.8	1.8	1.8	1.8	1.9	1.9
26.98	26.0	26.0	26.5	27.2	25.6	26.5	28.5	28.5
-	32.2	32.7	33.3	34.0	33.0	33.5	34.0	33.7
44.69	42.0	43.0	43.5	44.5	44.0	43.3	42.5	42.3
**	**	**	**	**	**	**	**	**
**	**	**	**	**	**	**	**	**
**	**	**	**	**	**	**	**	**
**	**	**	**	**	**	**	**	**
**	**	**	**	**	**	**	**	**
**	**	**	**	**	**	**	**	**
**	**	**	**	**	**	**	**	**
**	**	**	**	**	**	**	**	**
**	**	**	**	**	**	**	**	**
**	**	**	**	**	**	**	**	**
**	-	-	-	-	-	-	-	-
**	-	-	-	-	-	-	-	-
**	-	-	-	-	-	-	-	-
0.0664	0.0972	0.0911	0.0941	0.0920	0.0895	0.0870	0.0972	0.0953
0.0690	0.0972	0.0912	0.0957	0.0938	0.0895	0.0871	0.0967	0.0938
0.0698	0.0971	0.0911	0.0953	0.0933	0.0900	0.0875	0.0970	0.0948
too rough	4	on rig	5	too rough	5	on rig	on rig	too rough
too rough	4	too rough	4 to 5	too rough	4 to 5	too rough	3	too rough

ing load)

B

low seal pressure differentials, but at higher pressure differentials, the leakage rates with speeds of 200 or 300 ft/sec are significantly higher than that for static conditions. It is also apparent that some difference exists for the two speeds at which testing was conducted, although the difference is small.

An attempt was made to test with a rubbing speed of 400 ft/sec, but excessive leakage occurred, and the test was terminated. Inspection revealed excessive seal wear, which necessitated removal of the rig. Test time at this point totalled 50 hours. Inspection of the disassembled rig revealed a groove approximately 0.010 inch deep in the wear track of the PWA-771 LC1C-coated seal plate. Carbon lip wear was approximately 0.025 inch which corresponds to the relatively high wear rate of 50 mils per 100 hours. Hardness testing of the seal plate indicated Rc hardness values of 69 in the groove, 67.5 on the surface, and 51 on the rear side. The specification for the material requires a hardness of Rc 48 to 55 for the base material and a hardness of Vickers 650 to 1000 (Rc 58 and higher) for the LC1C hardface. The appearance of the Build 2 components after testing is shown in Figures 31, 32, and 33.
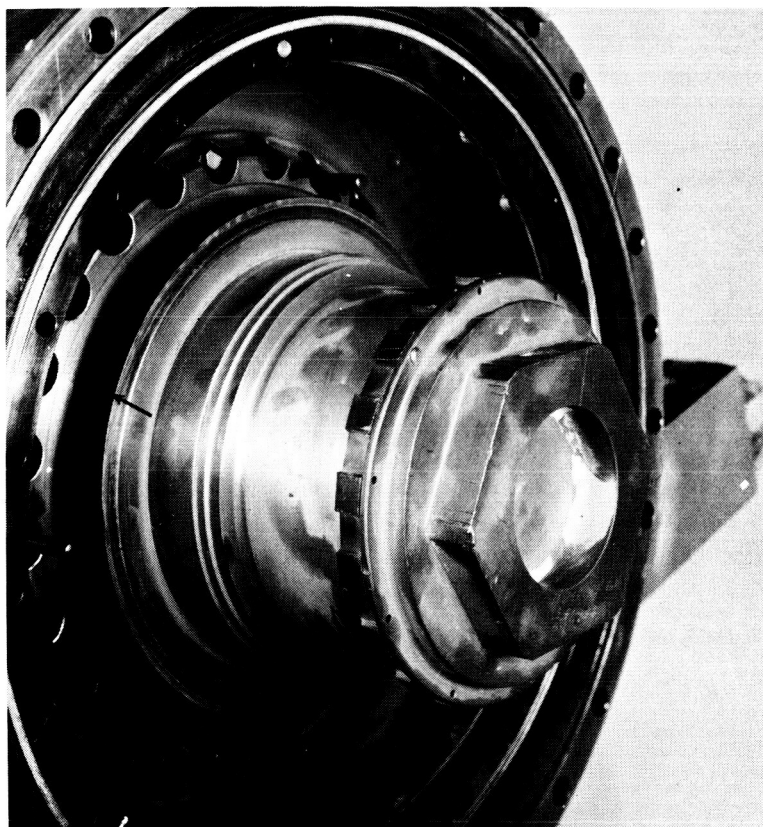
Figure 31   Carbon Face Seal With Piston Ring Secondary Seal Rig Hub After 50 Hours of Simulated Engine Operation With Air at 800°F and Oil at 250°F (Build 2) Showing Carbon Wear Track on Seal Plate Hardface (Linde LC1C)   XP-67042

PWA-2996
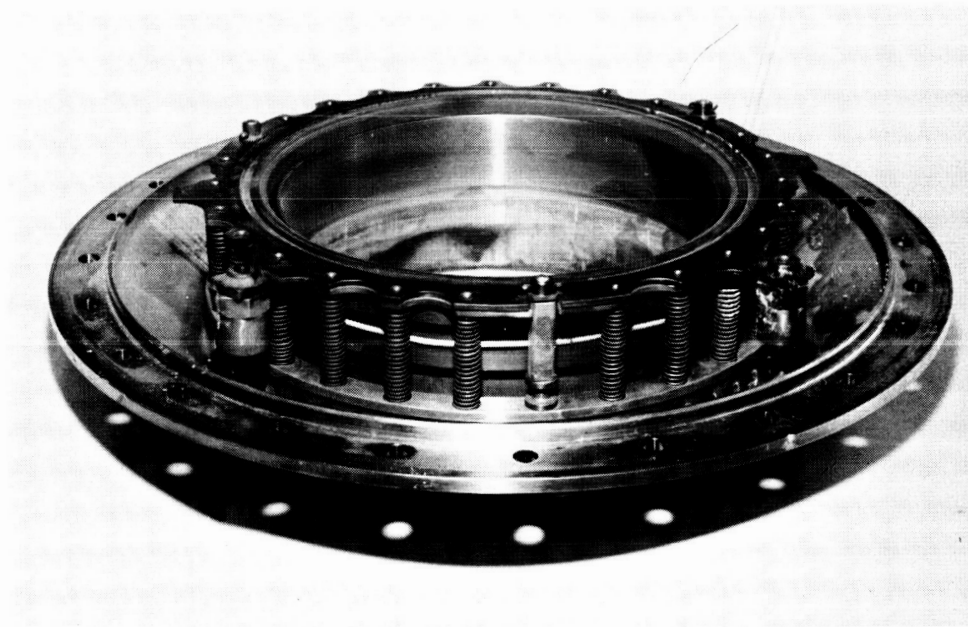
Figure 32   Carbon Face Seal With Piston-Ring Secondary Seal After 50 Hours
             of Simulated Engine Operation With Air at 800°F and Oil at 250°F
             (Build 2)   XP-67041

Figure 33   PWA 771 Seal Plate With LC1C Hardface After 50 Hours of
             Simulated Engine Operation Against Carbon Face Seal With Piston-
             Ring Secondary Seal With Air at 800°F and Oil at 250°F (Build 2).
             Note Groove Worn Through Hardface in Carbon Seal Wear Track
                                                                          XP-67180

Build 3 - The third build was completed on August 26, 1966. This build incorporated a new carbon seal assembly and the seal plate from Build 1, which had been re-lapped and modified to provide larger oil cooling holes. In addition, Build 3 incorporated an oil spray manifold to direct cooling oil at the rear side of the carbon seal carrier. The build was run for 5.75 hours, but excessive leakage occurred at seal pressure differentials above 120 psig (see Figure 34). Post-test inspection of the carbon seal assembly revealed deterioration of the carbon lip surface. The lip wear was 6.0 mils after only 5.75 hours of running. Inspection of the seal assembly dimensions revealed that the carbon lip outer diameter was 0.036 inch above the specified size, which resulted in a geometric area ratio unbalance of 0.57 instead of the required 0.65. The appearance of the seal after testing is shown in Figures 35 and 36.
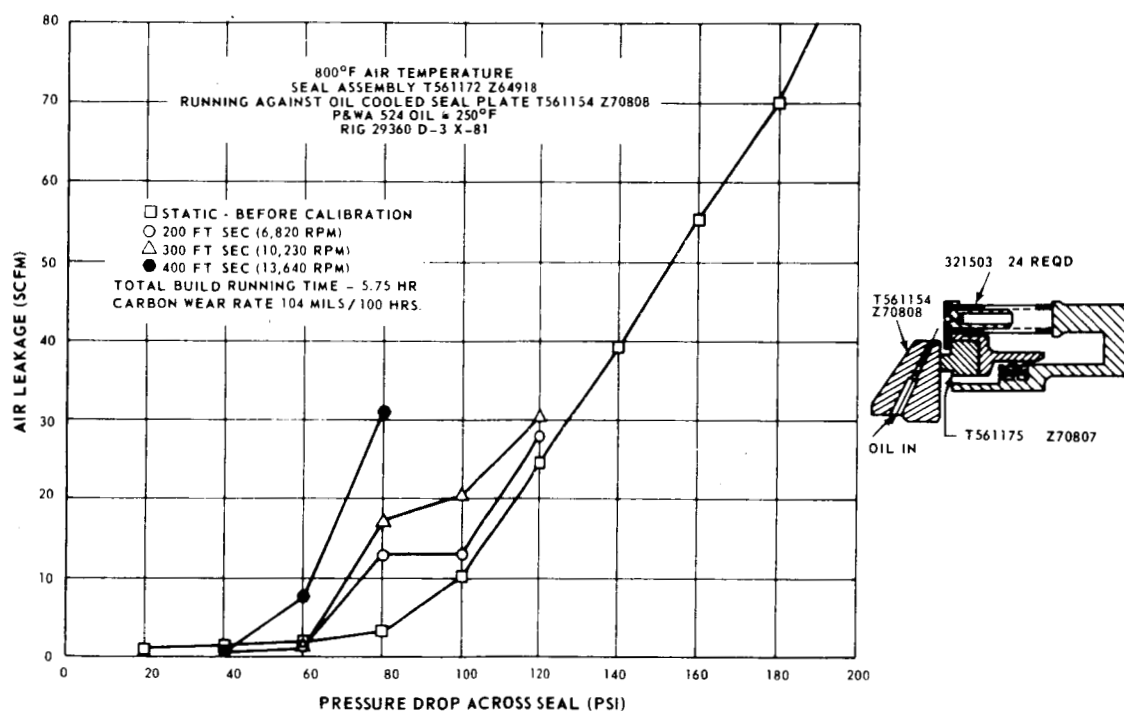
Figure 34   Leakage Calibration Results for Carbon Face Seal With Piston-Ring Secondary Seal (Build 3)
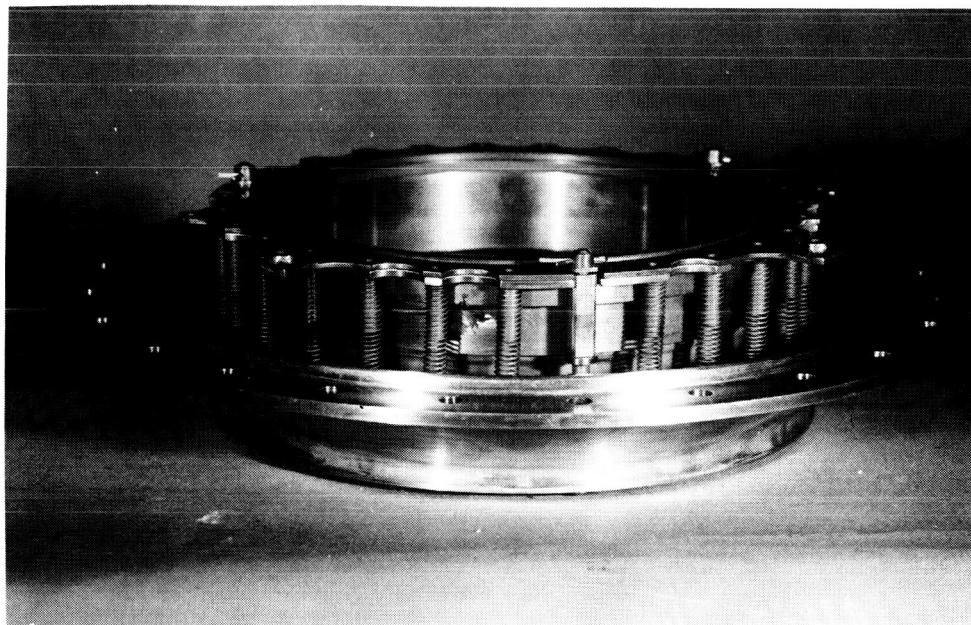
Figure 35   Carbon Face Seal With Piston-Ring Secondary Seal After 5.75 Hours
of Simulated Engine Operation With Air at 800°F and Oil at 250°F
(Build 3)   XP-68386
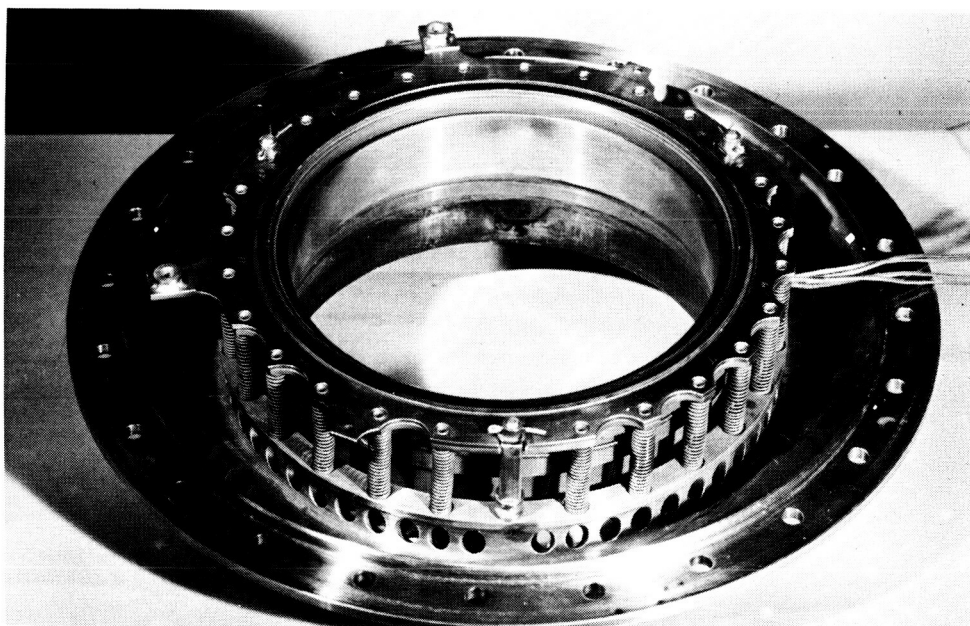
Figure 36   Carbon Face Seal With Piston-Ring Secondary Seal After 5.75 Hours
of Simulated Engine Operation With Air at 800°F and Oil at 250°F
(Build 3)   XP-68387

Build 4 - Subsequently, the carbon seal lip was machined to the proper dimensions, lapped, and reinstalled in the rig. Testing was resumed on Build 4, and the results obtained are shown in Figure 37. The seal performed well for 9.75 hours when an abnormal increase in air leakage rate caused the breather temperature and pressure to increase excessively. At the time of the increase, the seal was being tested at a rubbing speed of 400 ft/sec, a pressure differential of 160 psi, air at 1000°F, and oil at 325°F. Post-test examination revealed that the carbon lip surface was in an unsatisfactory condition. Carbon wear was 2 mils for 9.75 hours of testing. The seal plate also showed some signs of wear in the carbon lip wear track. The appearance of the seal assembly after Build 4 testing is shown in Figures 38 and 39.
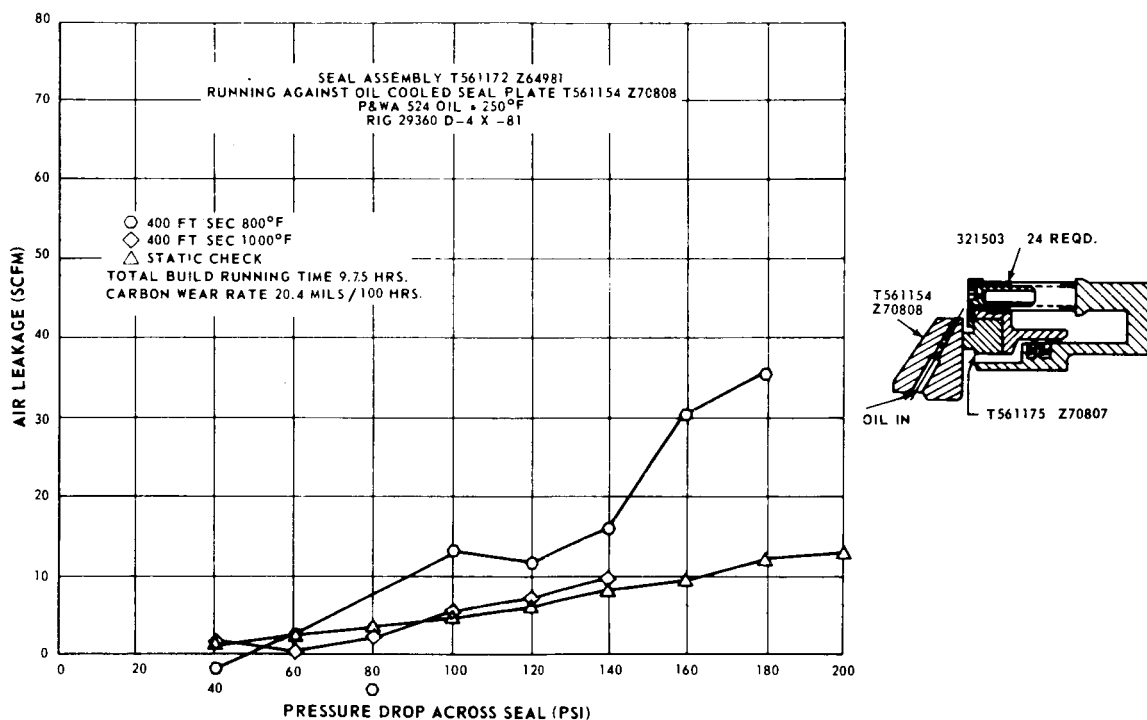
Figure 37   Leakage Calibration Results for Carbon Face Seal With Piston-Ring Secondary Seal (Build 4)

Figure 38   Carbon Face Seal With Piston-Ring Secondary Seal After 9.75 Hours
             of Simulated Engine Operation (Build 4)   XP-68849
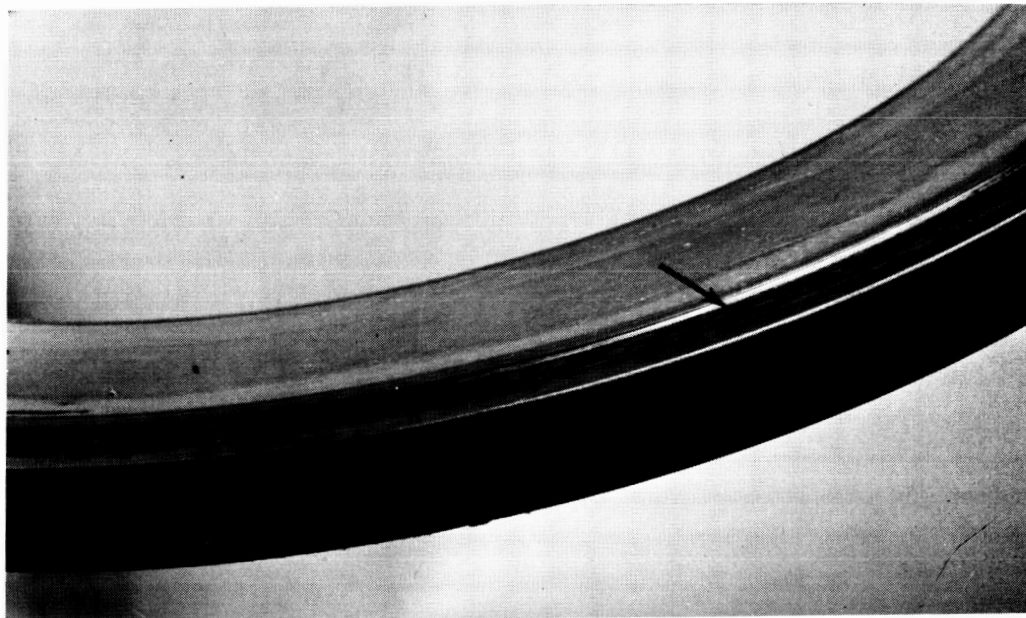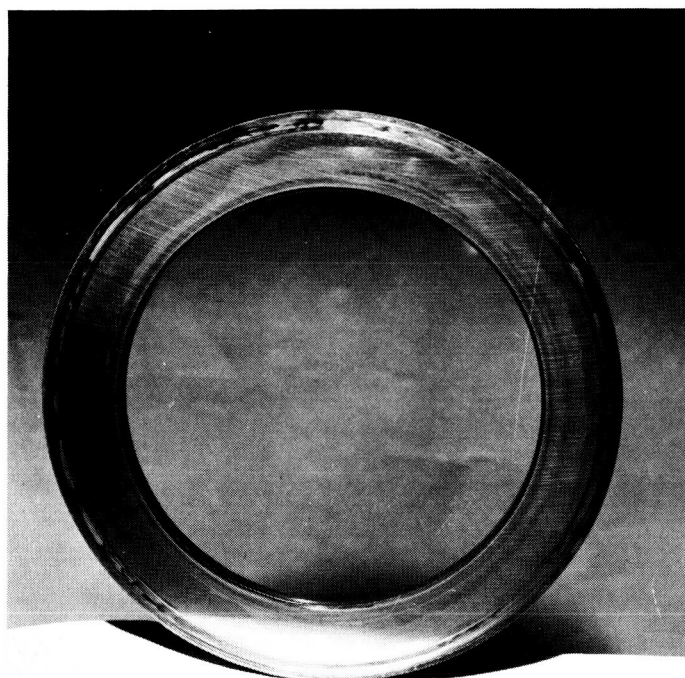

Figure 39   PWA 771 Seal Plate With LC1C Hardface After 9.75 Hours of
             Simulated Engine Operation Against Carbon Face Seal With Piston
             Ring Secondary Seal (Build 4)   XP-68850

Build 5 - The carbon seal assembly and seal plate from Build 4 were relapped and re-installed in the test rig. Also, an oil jet to supply additional cooling oil to the front rig roller bearing was installed. The under-race cooling oil flow to the roller bearing inner race and seal plate oil scoop was increased from 15 ppm to 24 ppm. Testing of Build 5 was started on October 27, 1966. This build was tested with an inlet air temperature of 1200°F, and the results are shown in Figure 40. A total of 14.75 hours of operation was accumulated on this build before testing was terminated by excessive seal air leakage. The conditions at the last point were a rubbing speed of 300 ft/sec, a pressure differential across the seal lip of 40 psi, inlet air temperature of 1230°F, and oil at 215°F. Air leakage was 32.2 scfm.

Post-test examination revealed that the carbon lip was slightly scored and that the carbon lip wear was 2.5 mils for the 14.75 hours of test time. The carbon seal assembly moved freely in the carrier and showed no evidence of excessive piston ring friction. However, the seal assembly air leakage in the pressure test fixture at 80 psi was 5.8 scfm. Consequently, the carbon lip profile was examined in the metrology laboratory. It was found that the surface was approximately 0.00050 inch out of flat. The surface had assumed a conical shape with the outside edge an average of 0.00045 inch higher than the inside edge. The seal plate was in good condition, although the carbon lip wear track was polished with small amounts of carbon-varnish deposits.

Build 6 - The last build tested during the report period employed a new carbon seal assembly and the same seal plate used for Build 5. Testing was conducted at a rubbing velocity of 300 ft/sec with oil at 250°F. Seal air pressure differentials up to 200 psi were used, and the air temperature was increased from 800 to 1200°F during testing at each pressure level. Test results are shown in Figure 41. As shown, the seal leakage increased sharply when the temperature was increased from 800°F to 1200°F at pressures above 100 psi. At 800°F, the seal performance was marginal at pressures of 200 psi and above. At 1000°F, performance became marginal at 140 psi, and at 1200°F, performance became marginal at 120 psi.

Following these tests, the seal assembly was removed from the test rig for inspection prior to testing with an oil temperature of 450°F. Static leakage of the assembly at 80 psi revealed a leakage rate of 2.85 scfm. Inspection of the carbon seal face found it in good condition with wear of 2.2 mils for the 101.75 hours of test time accumulated. The seal plate wear track was polished with small amounts of carbon varnish deposits and a slight depression (0.0005 in. deep) was found in part of the carbon wear track.
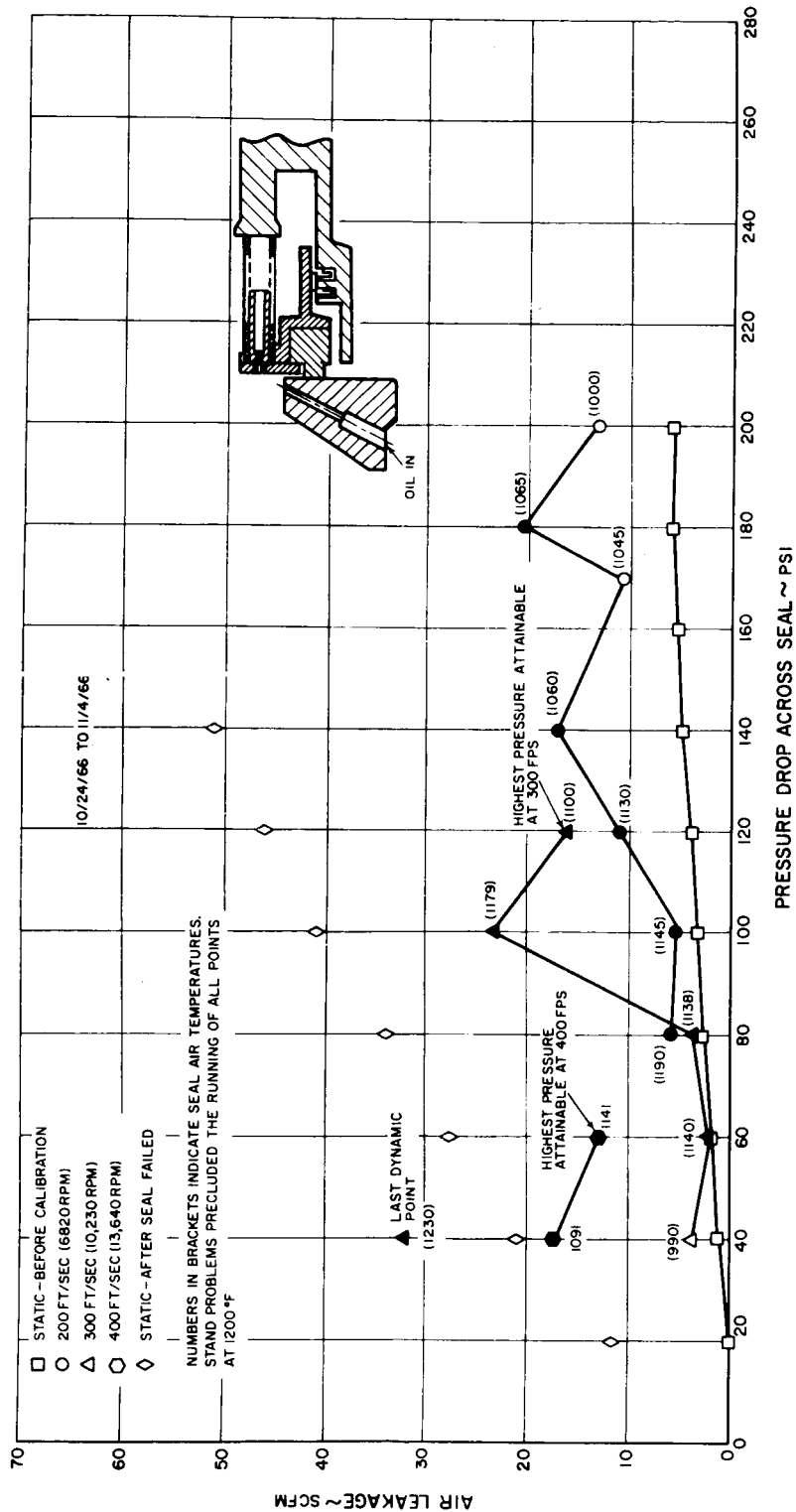
Figure 40   Leakage Calibration Results for Carbon Face Seal With Piston–
Ring Secondary Seal (Build 5)
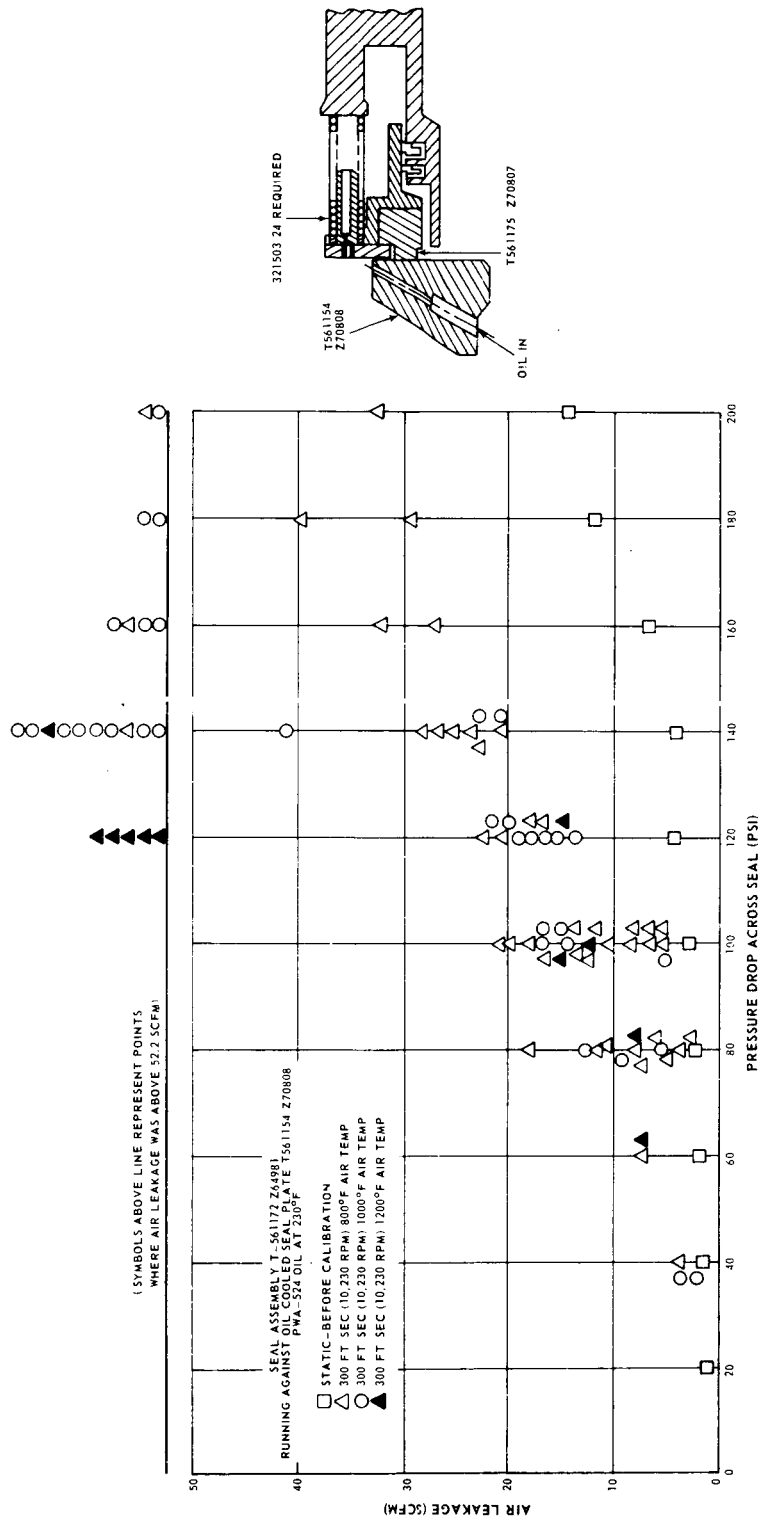
Figure 41   Leakage Calibration Results for Carbon Face Seal With Piston-Ring Secondary Seal (Build 6)

b. ORIFICE-COMPENSATED HYDROSTATIC FACE SEAL

Seven builds of the orifice-compensated hydrostatic face seal have been tested,
all within the current six-month report period. The results of testing each
build are summarized in Table IV, and pretest and post-test inspection data are
summarized in Table V.

Build 1 - Testing of the first build was started in August 1966. Static leakage was
72 scfm at 60 psi, which is excessive, and running the seal at a rubbing velocity
of 160 ft/sec for one hour and 240 ft/sec for one-half hour using air at room temp-
erature at pressures up to 60 psi did not reduce the leakage rate. The static leak-
age rates recorded by the Stein Seal Company after testing of this build are shown
in Figure 42. Inspection of the seal plate revealed that the outer edge of the carbon
seal face had been rubbing against the seal plate. Subsequently, the Stein Seal
Company performed a static pressure test and found the leakage to be considerably
less than that measured in the test rig.
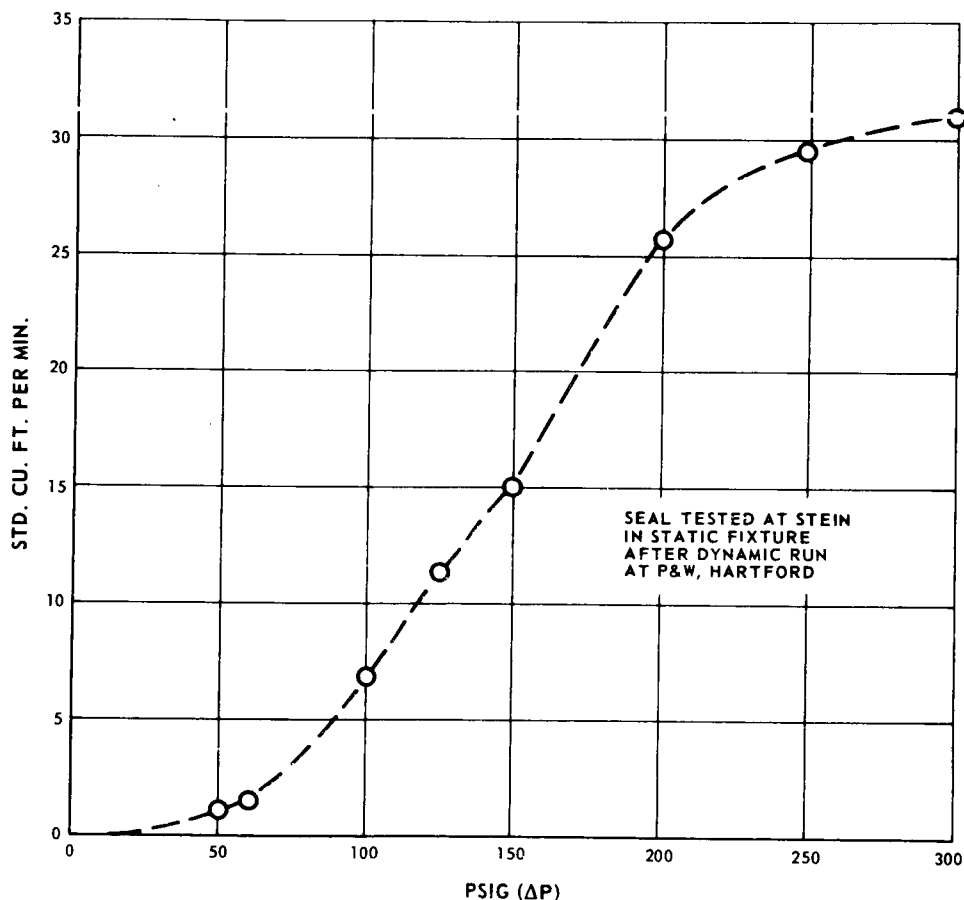
Figure 42   Leakage Calibration Results for Orifice-Compensated Hydrostatic
             Seal (Build 1)

ORIFICE COMPENSATED HY

Build No.	Seal Plate	Carbon Seal	Other Special Features	PCO	SEO	20 Hr. E
1	New	New - carbon lip design incorrect	T/C's connected to seal	X		
2	Used - from Bld. 1	Used - from Bld. 1 carbon lip design incorrect	No T/C's connected to seal	X		
3	Used - from Bld. 2	Used - from Bld. 2 carbon lip design incorrect.	No T/C's connected to seal	X		
4	Used - from Bld. 3	New - correct carbon lip design.	No T/C's connected to seal	X		
5	New	New - correct carbon lip design	No T/C's connected to seal	X		
6	New spring loaded plate	New - correct carbon lip design	No T/C's connected to seal	X		
7	Used - from Bld. 6 spring loaded plate	Used - ex Bld. 6 relapped	No T/C's connected to seal	X		

PCO = Preliminary Check Out
SEO = Simulated Engine Operation

A

TABLE IV

DROSTATIC FACE SEAL TEST SUMMARY

| - Tests - | | | | Reason for | Condition After Test | | Test |
nd.	Cyc. End.	Max. Cap.	Inert Gas	Test Termination	Seal Plate	Carbon Seal	Hours
				Excessive leakage	Slight rubbing on outer lip	Good	1.5
				Excessive leakage	Good	Good	0
				Excessive leakage	Good	Good	4.25
				Excessive leakage	Good	Good	6.50
				Rub at 320 ft/sec and 80ΔP	Severe burn marks	Severe wear	6.00
				Rub at 400 ft/sec and 60 ΔP	Severe burn marks	Severe wear	7.30
				Rub at 400 ft/sec and 80 ΔP	Severe burn marks	Severe wear	5.41

B

ORIFICE-COMPENSATE
AND POST-TEST PERF

Build No.			1	1	2	2
Test Condition			Pre	Post	Pre	Post
		Units				
Static Seal Leakage						
At assembly -	80 psig	SCFM	--	D	--	D
At test stand -	20 psig	SCFM	29.4	A	32.6	A
	40 psig	SCFM	52.1	T	54.0	T
	60 psig	SCFM	72.2	A	73.1	A
	80 psig	SCFM	95.5		95.5	
	100 psig	SCFM	121.5	N	125.0	N
	120 psig	SCFM	139.2	O	>125	O
	140 psig	SCFM	>139.2	T	>125	T
	160 psig	SCFM	>139.2		>125	
	180 psig	SCFM	>139.2	T	>125	T
	200 psig	SCFM	>139.2	A	>125	A
	220 psig	SCFM	--	K	--	K
	240 psig	SCFM	--	E	--	E
	260 psig	SCFM	--	N	--	N
Spring Rate in Assembly		lb/in.	16.75			
Total Spring Force (no piston rings)						
Tare wt (Seal face assembly)		lb	3.44	Same as	Same as	Same as
Total Load (Normal assembled length)		lb	4.25	Build	Build	Builds
Total Load (Operating length)		lb	5.3	1	1	1 and
Total Load (Fully compressed)		lb	8.4			2
Hydraulic Loading from Seal Unbalance of Test Stand with Springs and Piston Rings Installed						
	20 psig	lb	*		*	
	40 psig	lb	*		*	
	60 psig	lb	*		*	
	80 psig	lb	*		*	
	100 psig	lb	*		*	
	120 psig	lb	*		*	
	140 psig	lb	*		*	
	160 psig	lb	*		*	
	180 psig	lb	*		*	
	200 psig	lb	*		*	
	220 psig	lb	--		--	
	240 psig	lb	--		--	
	260 psig	lb	--		--	
Carbon Dam Height						
	0°	in.	0.0550	--	Same Seal	0.0550
	90°	in.	0.0549	--	as	0.0547
	Avg	in.	0.0549	--	Build 1	0.0549
Flatness						
Seal plate		He lt. bands	--	--	--	--
Carbon		He lt. bands	11	--	--	--

*Data not taken – await validation rig study

A

TABLE V

HYDROSTATIC FACE SEAL PRETEST
RMANCE AND INSPECTION SUMMARY

3 Pre	3 Post	4 Pre	4 Post	5 Pre	5 Post	6 Pre	6 Post	7 Pre	7 Post
--	D	--	D	2.8	--	2.8	--	3.92	--
3.4	A	1.8	A	≤1.7	2.6	1.1	9.2	1.0	13.2
7.1	T	5.2	T	3.4	13.2	2.6	26.0	1.9	32.8
12.7	A	7.5	A	5.3	36.0	4.5	52.0	2.5	56.2
18.2		11.0		6.9	48.6	5.8	80.0	4.7	87.8
28.5	N	17.2	N	10.5	82.6	7.5	106.3	5.9	102.0
37.5	O	24.0	O	13.0	108.8	8.7	>119	7.6	>119
45.8	T	28.2	T	19.0	>126.6	10.4	>119	9.3	>119
51.0		33.0		24.0	>126.6	13.6	>119	10.8	>119
59.3	T	38.0	T	27.8	>126.6	15.2	119	12.0	>119
67.3	A	44.2	A	34.0	>126.6	17.2	119	14.4	>119
--	K	--	K	--	--	--	--	--	--
--	E	--	E	--	--	--	--	--	--
--	N	--	N	--	--	--	--	--	--

16.75		13.35					•		

3.44	Same as	3.4	Same as	3.42	Same as	3.43	3.43	Same as	Same as
4.25	Builds	4.7	Build	Same as	Builds	Same as	Same as	Builds	Builds
5.3	1 and	5.6	4	Build	4 and	Builds 4	Builds 4	4, 5	4, 5
8.4	2	7.7		4	5	and 5	and 5	and 6	and 6

3 Pre	3 Post	4 Pre	4 Post	5 Pre	5 Post	6 Pre	6 Post	7 Pre	7 Post
*	*	*		*		*		*	*
*	*	*		*		*		*	*
*	*	*		*		*		*	*
*	*	*		*		*		*	*
*	*	*		*		*		*	*
*	*	*		*		*		*	*
*	*	*		*		*		*	*
*	*	*		*		*		*	*
*	*	*		*		*		*	*
	*								
--	--	--		--		--		--	--
--	--	--		--		--		--	--
--	--	--		--		--		--	--

0.0550	0.0551	0.0599	--	0.0613	Seal	0.0597	Seal	0.462	Seal
0.0547	0.0550	0.0598	--	0.0614	failed	0.0596	failed	0.461	failed
0.0549	0.0550	0.0598	--	0.0613		0.0596		0.461	

--	--	--	--	8	Seal	2 to 10	Seal	Checked	Seal
5	4	5	--	≤1	failed	≤2	failed	by Vendor	failed

B

Build 2 - In view of this result and the light spring loading on the seal assembly, it was thought that the thermocouple instrumentation could possibly have restrained the carbon seal from following the seal plate. Consequently, this instrumentation was omitted from Build 2. However, excessive air leakage still occurred at both static and dynamic conditions. Post-test inspection revealed that an auxiliary flange seal in the rig was contributing to the high leakage.

Build 3 - The rig seal problem was eliminated and testing of Build 3 was commenced in late September 1966. Static and dynamic leakage rates were still high, however, as shown in Figure 43. Inspection of the seal and seal plate revealed no damage or signs of wear.
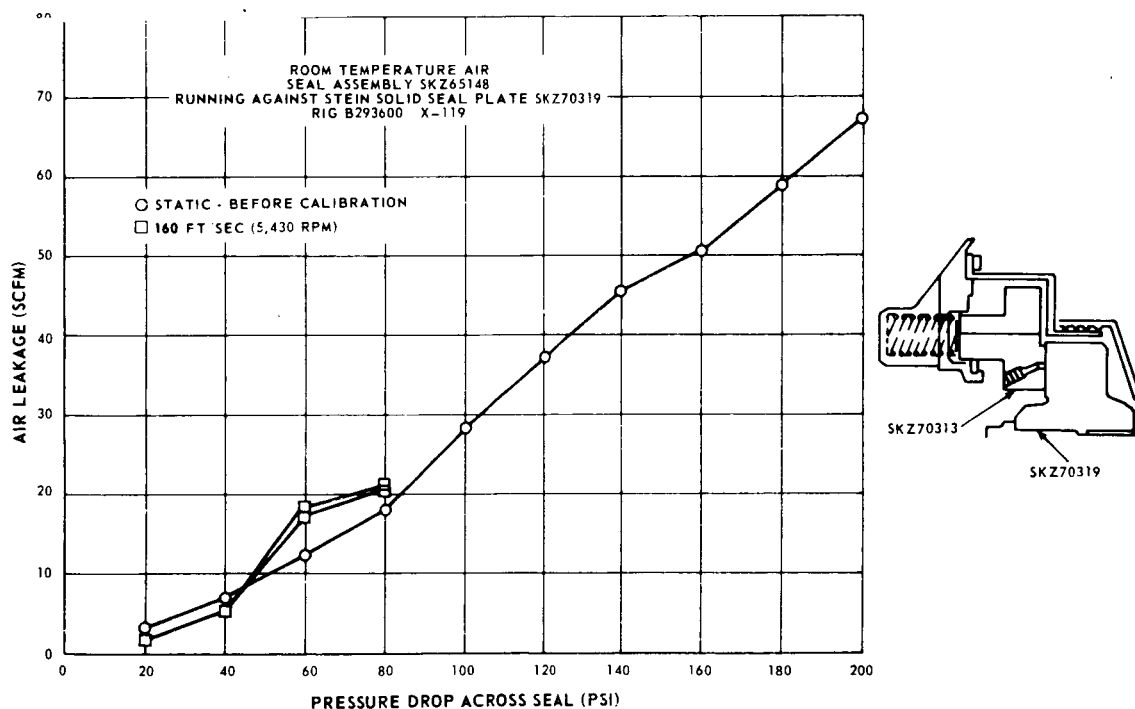
Figure 43   Leakage Calibration Results for Orifice-Compensated Hydrostatic Seal (Build 3)

Build 4 - For Build 4, the Stein Seal Company provided a new seal with a revised carbon lip which produced an improved restoring force characteristic when the seal moves from its design face opening clearance. The new seal was tested, but, as shown in Figure 44, leakage was still excessive. Inspection of the seal and seal plate revealed no damage to either component. The seal was then tested in the Pratt & Whitney Aircraft static-pressure test fixture. The leakage rate was significantly lower than in the rig. At a pressure of 80 psi, leakage in the test fixture was 3.2 scfm, whereas at the same pressure in the rig, the leakage had been 11.0 scfm. Subsequently, the Stein Seal Company conducted a static leakage calibration and obtained the following results:

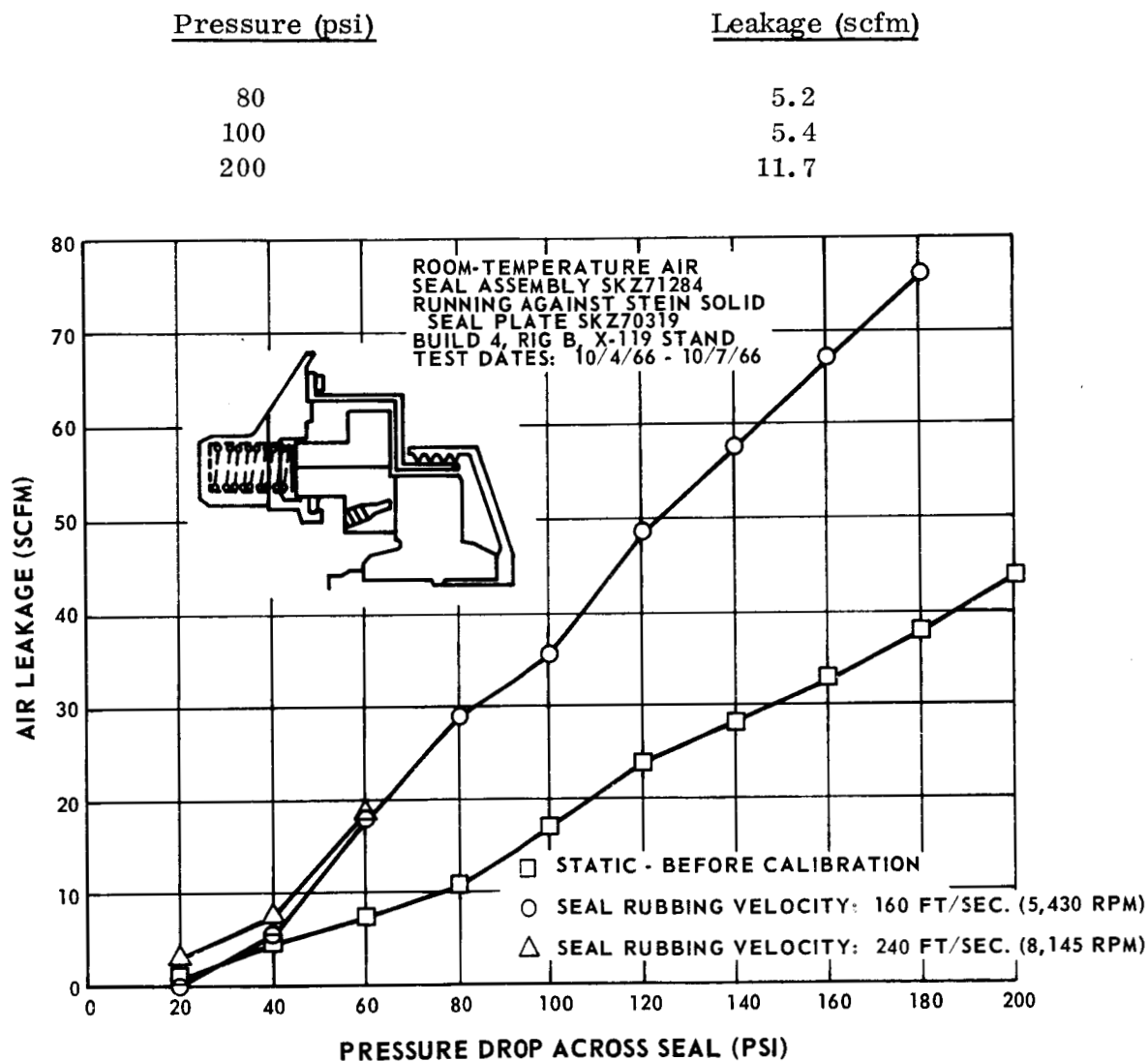| Pressure (psi)	Leakage (scfm)
80	5.2
100	5.4
200	11.7

Figure 44   Leakage Calibration Results for Orifice-Compensated Hydrostatic Seal (Build 4)

The seal plate was dimensionally inspected by means of an electro-probe. The peculiar shape of the seal plate precluded use of a standard optical flat. The face of the seal plate was found to be flat within 0. 000012 to 0. 000015 inch FIR, and to be conical with the outside edge 0. 000015 to 0. 000020 inch higher than the inside edge. This flatness was within the specified flatness of 0. 000020 inch FIR.

Since the face seal was found to meet specifications, the effect of assembly procedure was investigated. The seal plate and hub were assembled with the hub nut torqued to 2000 inch-pounds plus 30 to 35 degrees of rotation. The plate was then checked for flatness and was found to be out of flat by 0. 0008 to 0. 0010 inch FIR and to be conical with the outer edge being 0. 000040 to 0. 000080 inch higher than the inner edge. Subsequently, the flatness was checked with the hub nut torqued to 2000 inch-pounds plus 5 to 10 degrees of rotation. This procedure resulted in the plate being out of flat by 0. 00045 to 0. 00063 inch FIR and to be conical with the outer edge 0. 000040 to 0. 000060 inch higher than the inner edge.

Build 4 was also used to measure the static pressure profile in the orifice-annulus segments in the carbon seal lip. The probes were positioned 10, 30, and 50 degrees from the orifice holes, and pressures were measured with pressure differentials across the seal ranging from 20 to 200 psi. The results will be correlated with analytically predicted annulus pressures. The carbon seal ring and the assembled seal instrumented for these tests are shown in Figures 45 and 46, respectively.

Build 5 - For Build 5, a new seal plate and windback shroud were installed on the hub. The hub assembly was selectively stacked and the hub nut was torqued to 2000 inch-pounds plus 5 to 10 degrees of rotation. Following assembly, the seal plate was flat to within 0. 000074 to 0. 000090 inch and was conical with the outer edge 0. 000011 to 0. 000038 inch higher than the inner edge. A static leakage check in the rig, using air at ambient temperature and a pressure of 200 psi resulted in a leakage rate of 34. 0 scfm (see Figure 47). The first dynamic test was run at a rubbing speed of 160 ft/sec, and the leakage rate was 59. 8 scfm with a pressure differential of 200 psig. The second dynamic test was run at a rubbing speed of 240 ft/sec, and the leakage rate was 40 to 50 percent less than in the preceeding test at each pressure. The third test was run at 320 ft/sec and the leakage was negligible at a pressure differential of 60 psi (less than 1. 2 scfm). When the pressure differential was increased to 80 psi, however, the seal opened and the leakage increased suddenly to 41. 4 scfm. The test was terminated, and the seal was removed for inspection.

Inspection of the seal revealed a smooth lapped wear path on the outer lip of the carbon, whereas the inner lip was worn and rough. The outer edge of the seal plate face was polished, but the inner edge showed four, distinct, equidistant burn marks.
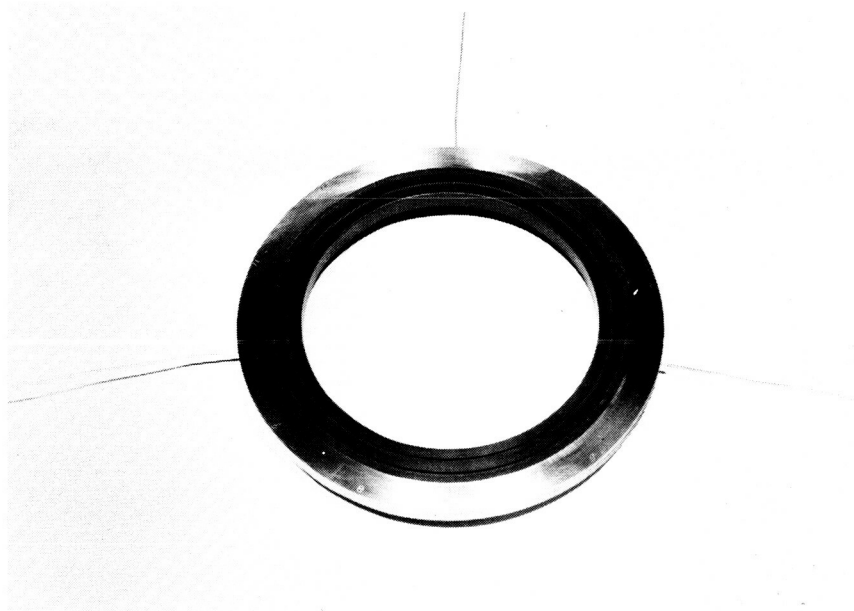
Figure 45   Carbon Seal Ring of Orifice-Compensated Hydrostatic Seal (Build 4)
Instrumented for Measuring Annulus Pressures   CN-7078

Figure 46   Orifice-Compensated Hydrostatic Seal (Build 4) Instrumented for
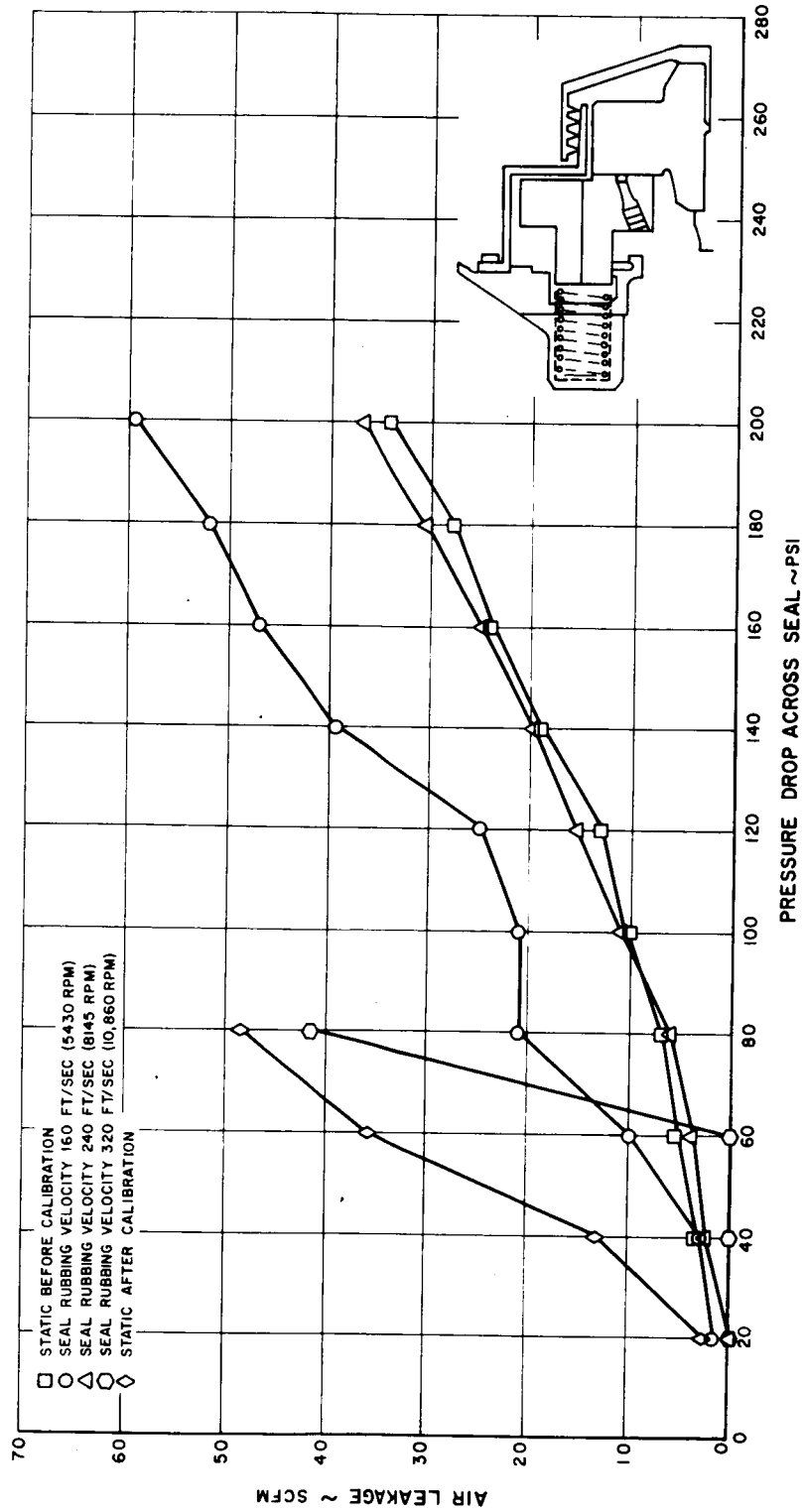Measuring Annulus Pressures   CN-7077

Figure 47   Leakage Calibration Results for Orifice-Compensated Hydrostatic Seal (Build 5)

Build 6 - Build 6 was completed during November 1966 and incorporated both the revised seal design and a new spring-loaded floating seal plate (see Figure 48). The seal plate hub assembly was checked for flatness and found to be flat within 0.000035 to 0.000045 inch and conical with the outer edge 0.00007 to 0.00009 inch higher than the inner edge. The carbon seal face was flat within 0.000020 inch and the seal plate runout was 0.002 inch.
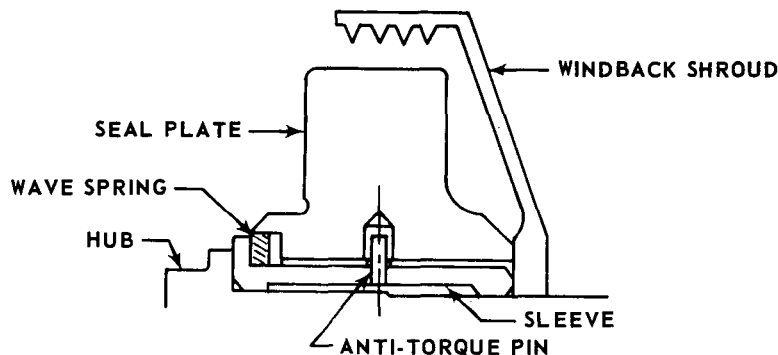
Figure 48   Stein Seal Company Spring-Loaded Floating Seal Plate Design

Static testing with a pressure differential of 200 psi and an ambient air temperature resulted in an air leakage rate of 17.2 scfm (see Figure 49). Dynamic testing with a rubbing speed of 160 ft/sec resulted in a leakage rate of 51.6 scfm at a pressure differential of 200 psig, and, at 300 ft/sec, the leakage rates at each pressure were approximately 50 percent of those obtained at 160 ft/sec. As the speed was being set for testing at 400 ft/sec with a pressure differential of 60 psi, however, the seal leakage suddenly increased to an excessive level. The test was terminated, and the hub and seal assemblies were removed for inspection. Inspection revealed essentially the same conditions as those found after testing Build 5. The assemblies were sent to the Stein Seal Company for inspection and refinishing as required.

Figure 49   Leakage Calibration Results for Orifice–Compensated Hydrostatic Seal (Build 6)

Build 7 - The Stein Seal Company relapped the carbon seal and seal plate, and these parts were incorporated into Build 7. The static leaka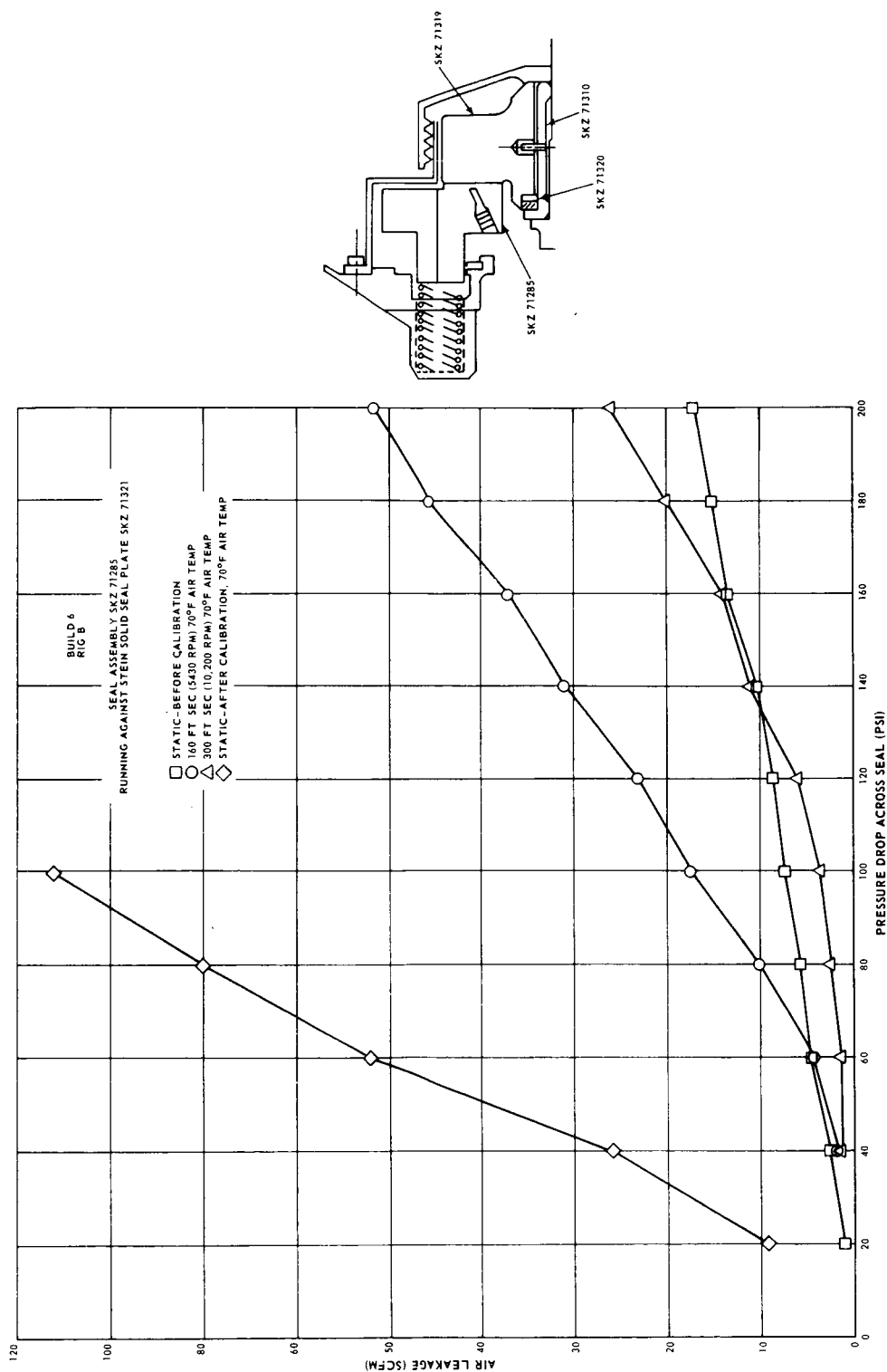ge test resulted in a leakage rate of 14.5 scfm at a pressure differential of 200 psi with ambient air temperature (see Figure 50). Dynamic testing at a rubbing speed of 400 ft/sec resulted in a leakage rate of 54.0 scfm with a pressure differential of 200 psi. Decreasing the pressure differential to 100 psi reduced the leakage rate to 27.0 scfm. The pressure differential was then reduced to 80 psi, but after about eight minutes, the leakage rate increased suddenly. A static check was performed, and the leakage for this condition was also excessive.

The seal was removed and inspected. The seal was found to have a smooth, lapped wear path on the outer lip of the carbon, but the inner lip was worn and rough. The outer edge of the seal plate face was polished, but the inner edge showed four, equidistant burn marks. Hence, this failure was essentially the same as that for Builds 5 and 6. The appearance of the seal components after Build 7 testing is shown in Figures 51 and 52.

c. INSTRUMENTATION VALIDATION RIG

Testing is being conducted to develop instrumentation for measuring seal wear without disassembling the rig and to measure seal torque during testing. The method being studied to measure seal wear involves measuring the displacement of the seal loading pistons with Bently probes. For the first test, the rig was run for 16.75 hours at a rubbing speed of 300 ft/sec and a pressure differential of 20 psi, with the air at ambient temperature. The probe data indicated zero wear, with an accuracy of 1 mil because of piston vibration. The actual wear was 0.2 mil. After running for 14.50 hours at a rubbing speed of 400 ft/sec and the same pressure differential and air temperature, one probe indicated a seal wear of 3.4 mils, the second indicated 10.3 mils, and the third was inoperative. Actual wear was 0.2 mils. The inconsistencies were caused by vibration of the pistons when they were in contact with the seal. The vibrations varied in amplitude to a maximum of 10 mils at frequencies considerably below the rig speed. Increasing the spring preload reduced the peak vibration amplitude to 6 mils and increased the vibration frequency to rig speed. Consequently, stiffer springs will be installed when they are available.

The rig was then run at a rubbing speed of 200 ft/sec with ambient air temperature and pressure differentials ranging from 20 to 200 psi. It was found that the total displacement of the cylinders was dependent on the seal air pressure, apparently because of axial displacement of the rig bearing with changing thrust load. With a seal pressure differential of 20 psi, the average travel was 27.6 mils, whereas with a seal pressure differential of 200 psi, the average travel was 20.0 mils. The movements of the three pistons, however, were within 1 mil of each other at all times. Considerable additional experimentation will be required to develop this technique to an acceptable level of accuracy.

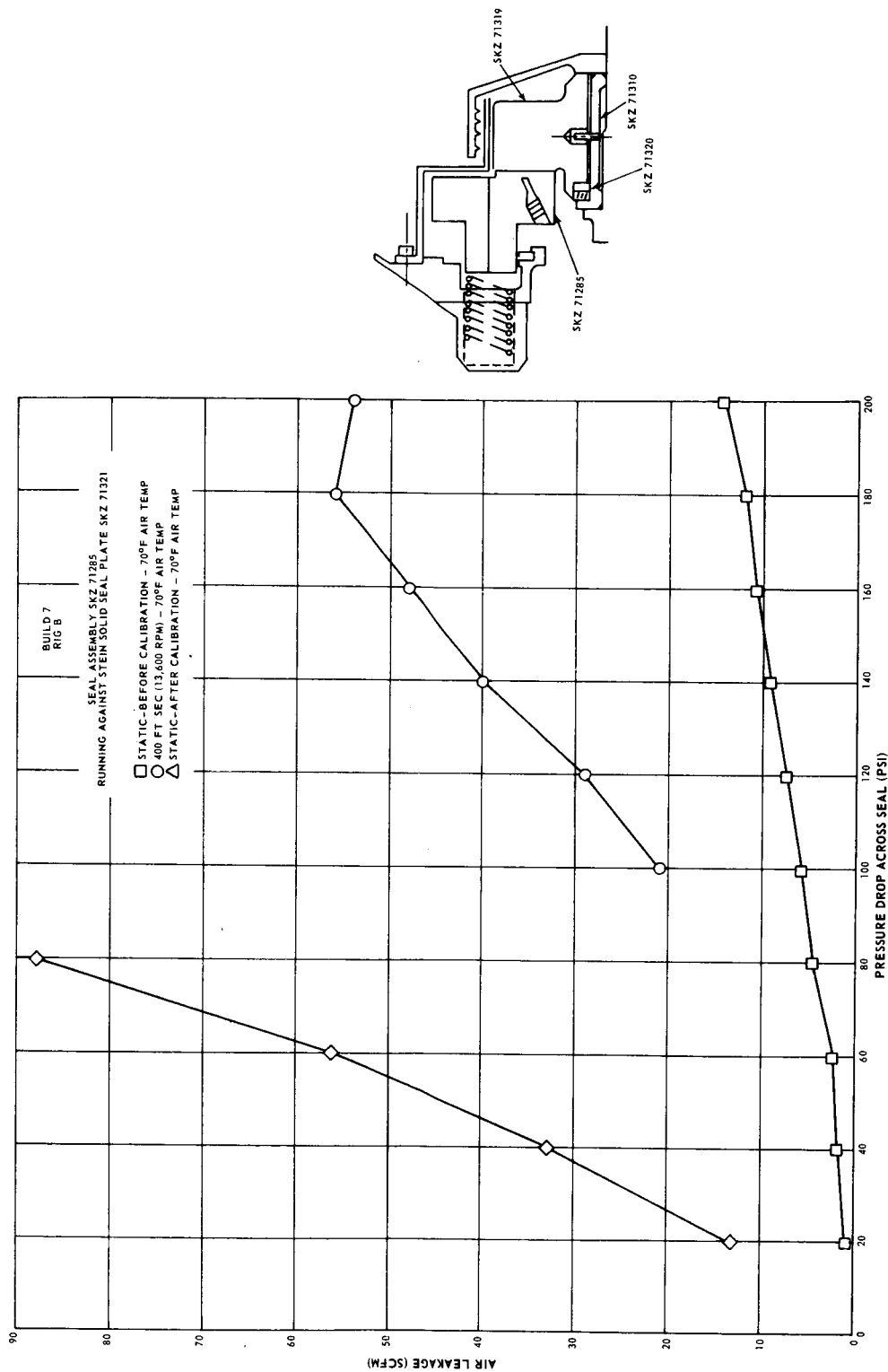Figure 50   Leakage Calibration Results for Orifice-Compensated Hydrostatic Seal (Build 7)
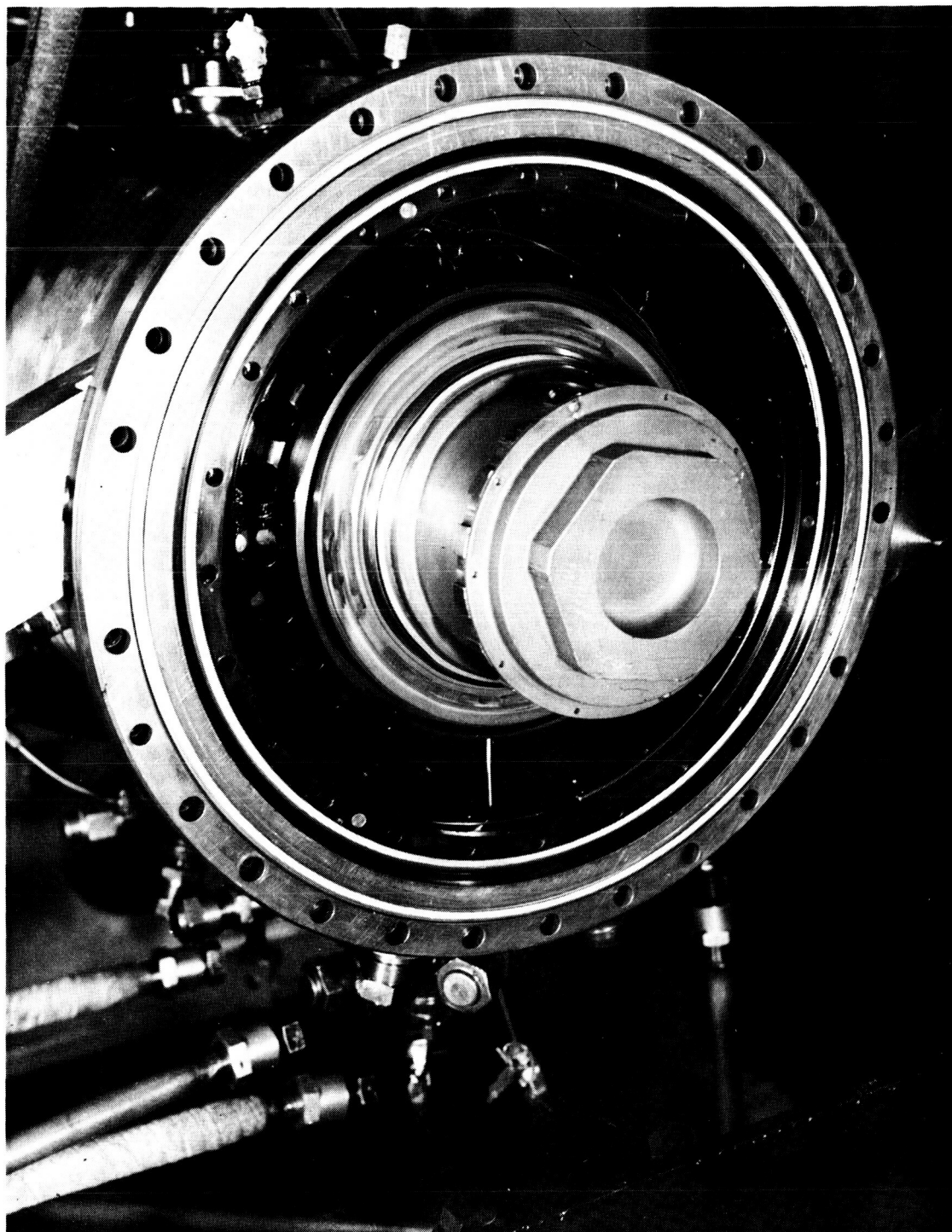
Figure 51   Orifice-Compensated Hydrostatic Seal Hub Assembly After 5.50
Hours of Build 7 Testing
Note Burn Marks on Seal Plate Hardface   CN-7422
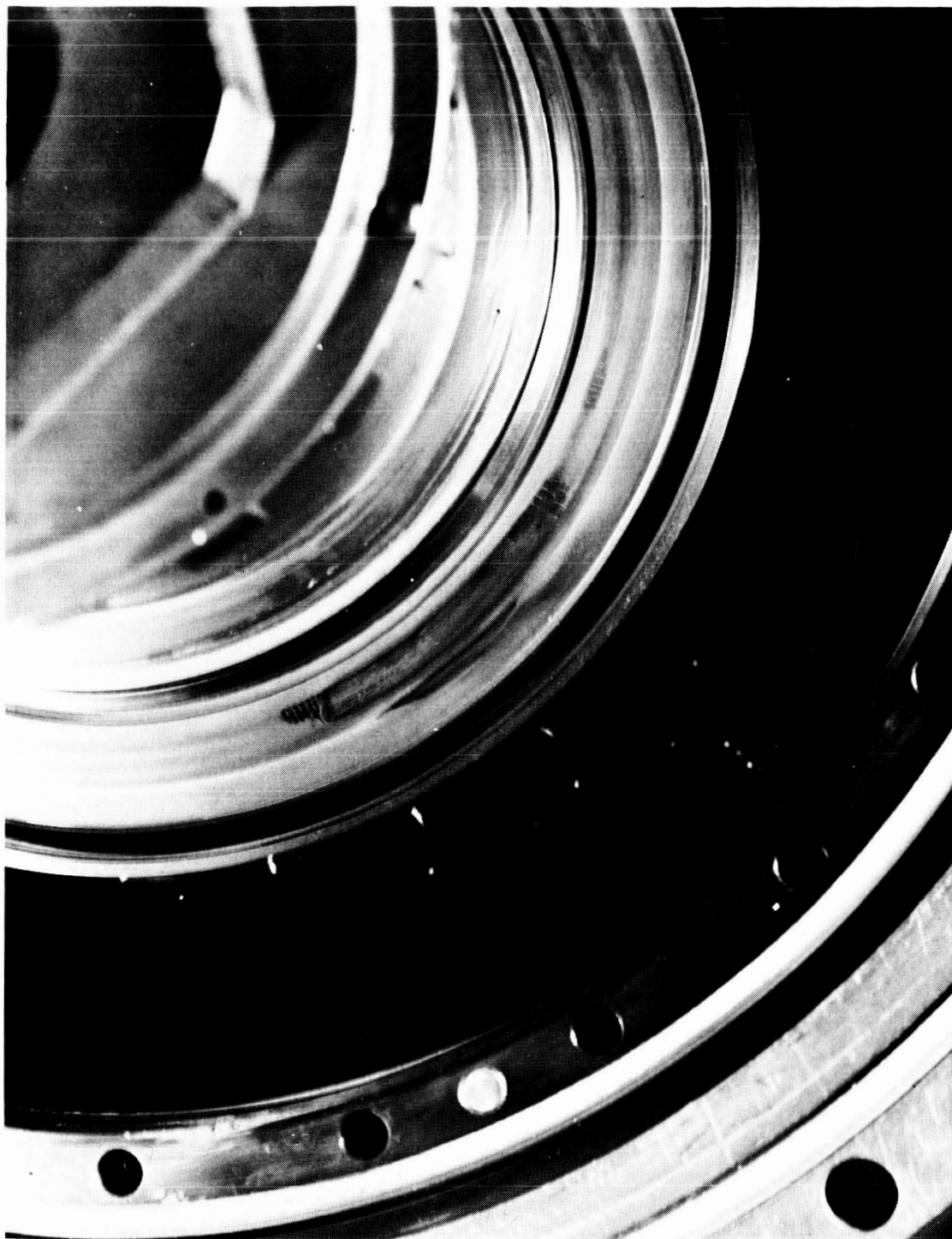
Figure 52   Orifice-Compensated Hydrostatic Seal Hub Assembly After 5.50
Hours of Build 7 Testing   CN-7423

Initial attempts to use the torque measuring device revealed that the transducers being used were too large. The transducers had a range of 0 to 100 lb, whereas the measured loads were on the order of 3 lb. In addition, vibration introduced errors in the transducer readings. An attempt was made to eliminate the vibration problem by deadweight loading the force arms. Testing, however, revealed that the deadweight loads had not been distributed equally between the two force transducers. The vibration was still excessive, and some of the vibration was being caused by the deadweight cable system. An attempt will be made to balance the loads between the transducers, and the transducer mounting system will be changed to reduce vibration. In addition, new transducers with a smaller load range will be procured.

APPENDIX

Externally Pressurized Hydrostatic
Seal Design Drawings

Figure 53   Externally Pressurized Hydrostatic Seal Assembly (Stein Seal Co.
No. 2991-P1)

Figure 54   Seal Carrier for Externally Pressurized Hydrostatic Seal (Stein
Seal Co. No. SSCY 2993-1)
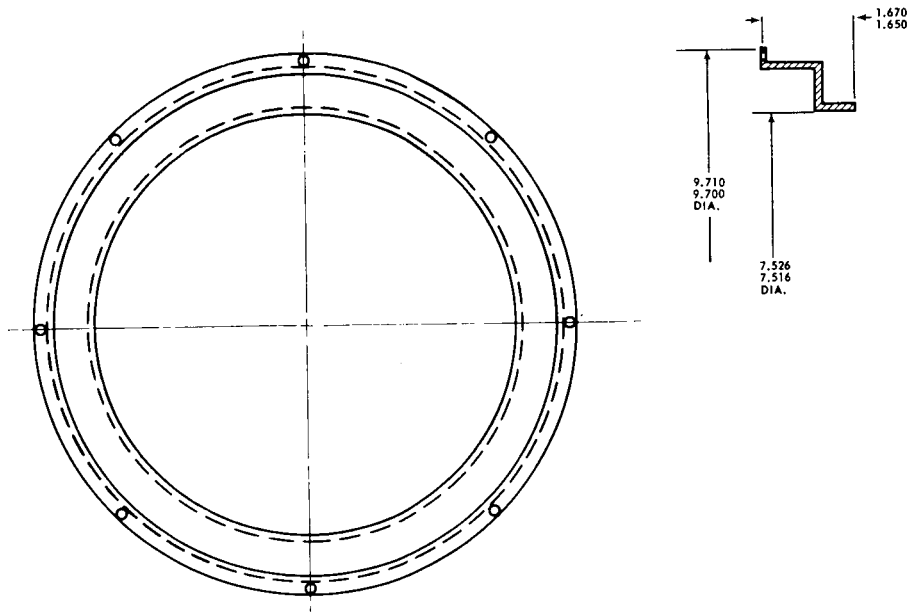
Figure 55   Assembly Guard for Externally Pressurized Hydrostatic Seal
(Stein Seal Co. No. SKZ 70716-C)

Figure 56   Seal Assembly for Externally Pressurized Hydrostatic Seal (Stein
Seal Co. No. SSCY 2998)

Figure 57   Steel Band for Externally Pressurized Hydrostatic Seal (Stein Seal Co. No. SSCY 2998-1)

Figure 58   Seal Ring for Externally Pressurized Hydrostatic Seal (Stein Seal Co. No. SSCY 2998-2)

7.990
7.980
DIA.

5.154
5.152
DIA.

1.070
1.050

Figure 59   Shroud Windback for Externally Pressurized Hydrostatic Seal
(PWA No. SKZ 70714-C)

0.0805
0.0780

0.162
0.156

6.312
6.310
DIA

A

A

EXPANDED
SECTION A-A

Figure 60   Piston Ring (Large Diameter) for Externally Pressurized Hydrostatic
Seal (Stein Seal Co. No. SSCY 299304)
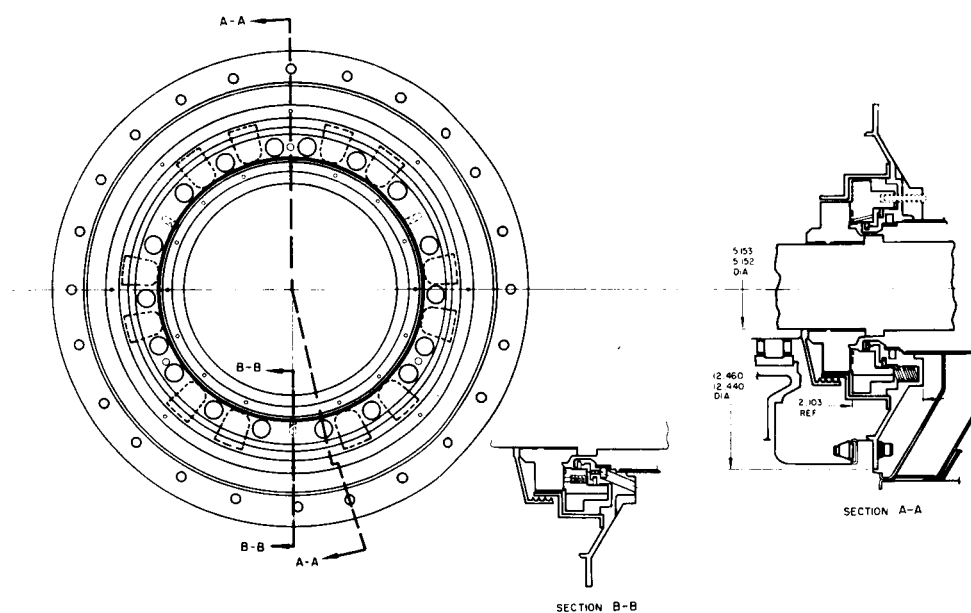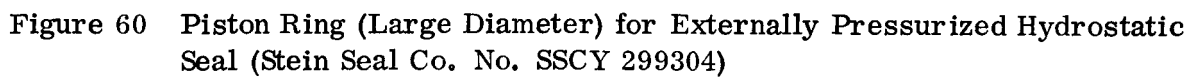
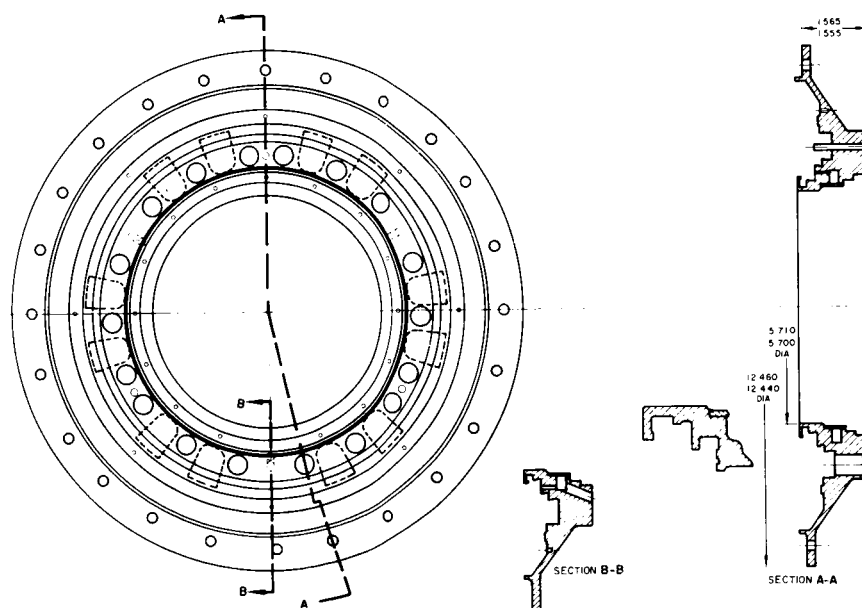Figure 61   Piston Ring (Small Diameter) for Externally Pressurized Hydrostatic
             Seal (Stein Seal Co. No. SSCY 2993-5)

Figure 62   Seal Plate for Externally Pressurized Hydrostatic Seal (PWA No.
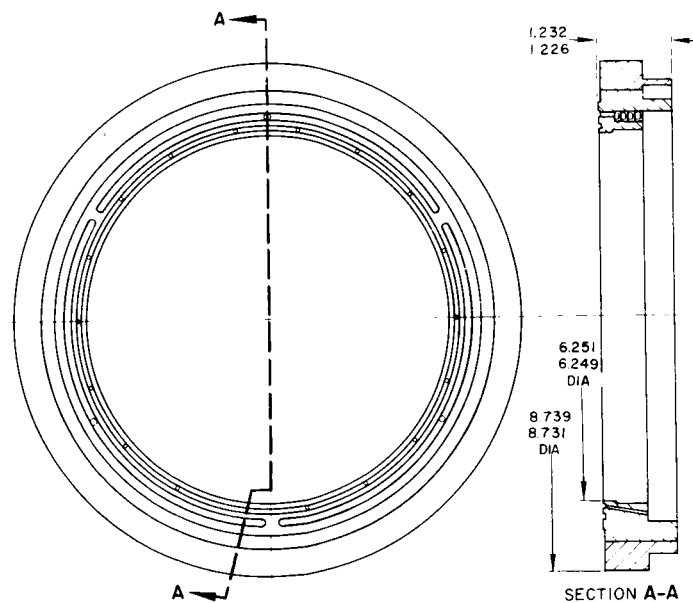   SKZ 70711-C)
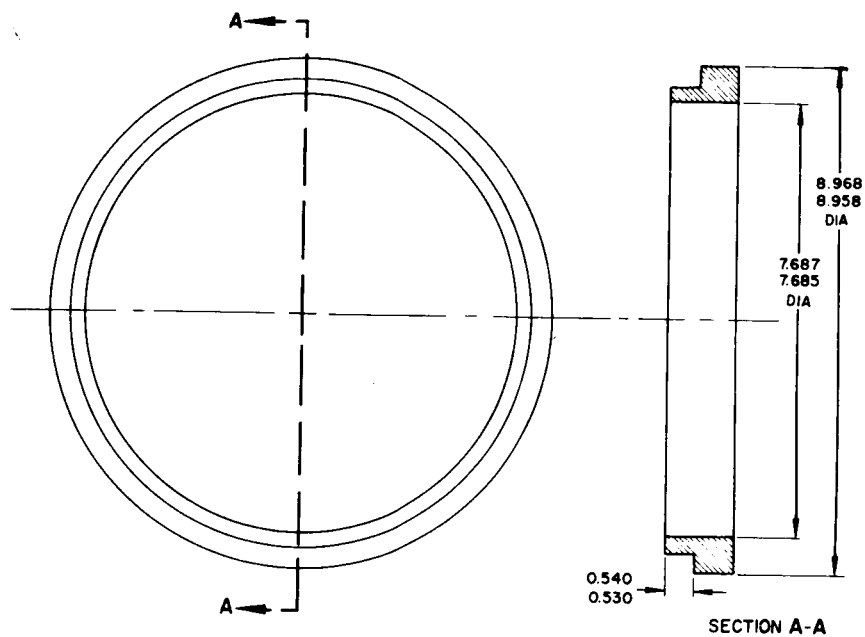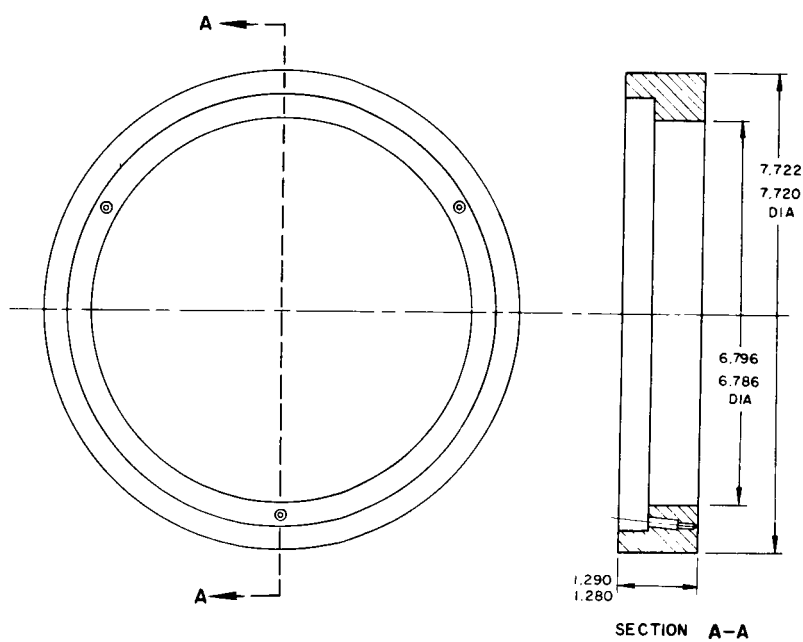
0.130
0.126
DIA

0.092
0.088

0.173
0.169
DIA

Figure 63   Orifice for Externally Pressurized Hydrostatic Seal (Stein Seal Co.
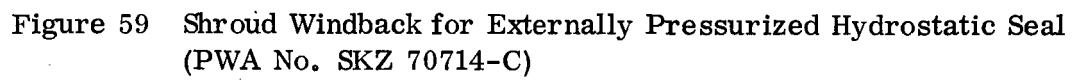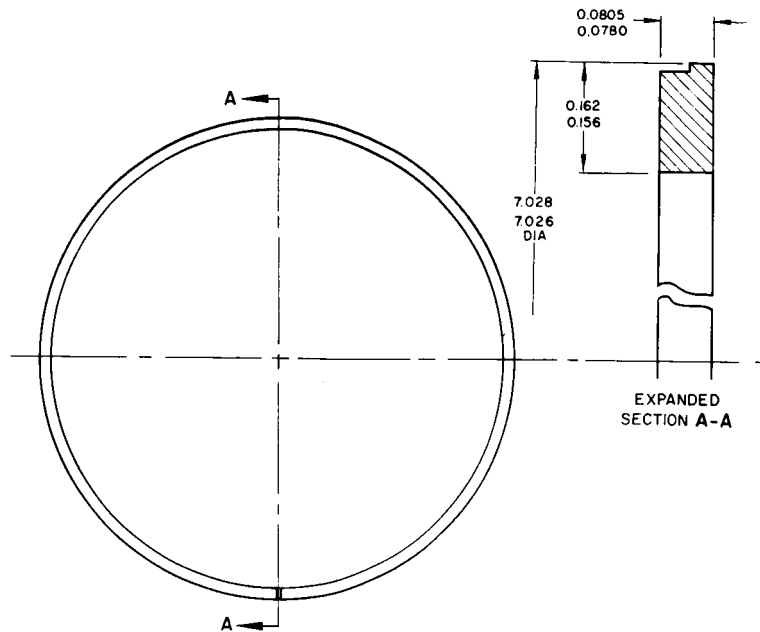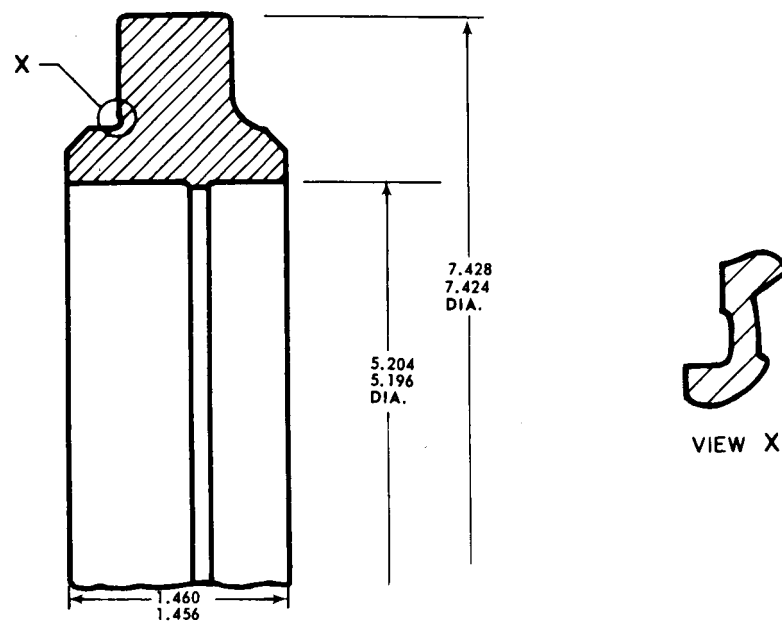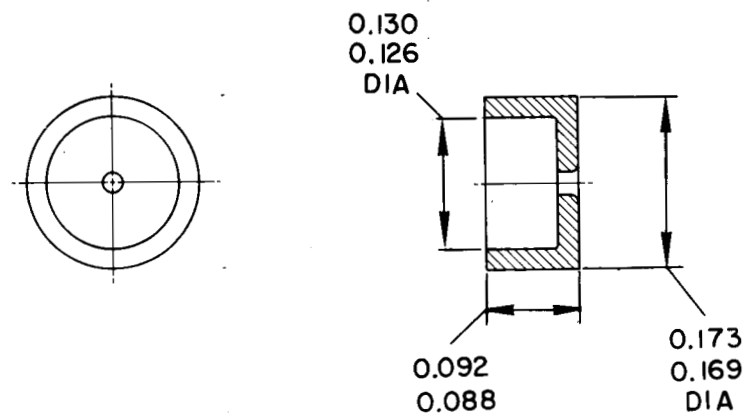No.   SSCY 2998-3)

Semiannual Reports

Distribution List
NAS3-7609

To:		Number of Copies	To:	Number of Copies
NASA-Lewis Research Center Air-Breathing Engine Procurement Section Attention: John H. DeFord		2	U. S. Naval Research Laboratory Washington, D. C. Attention: Charles Murphy	1
NASA-Lewis Research Center Air-Breathing Engine Division Attention: J. Howard Childs W. H. Roudebush D. P. Townsend Lawrence E. Macioce	M.S. 60-4 M.S. 60-6 M.S. 60-6 M.S. 60-6	1 1 4 1	Department of the Navy Bureau of Naval Weapons Washington, D. C. Attention: A. D. Nehman, RAAE-3 C. C. Singletorry, RAPP-4	1 1
NASA-Lewis Research Center Technology Utilization Office Attention: John Weber		1	Department of the Navy Bureau of Ships Washington 25, D.C. Attention: Harry King, Code 634A	1
NASA-Lewis Research Center Report Control Office		1	U. S. Navy Marine Engineering Laboratory Friction and Wear Division Annapolis, Maryland	
NASA-Lewis Research Center Attention: Library		1	Attention: R. B. Snapp	1
NASA-Scientific and Technical Information Facility Box 5700 Bethesda, Maryland Attention: NASA Representative		6	Department of the Army U. S. Army Aviation Material Labs. Fort Eustis, Virginia 23604 Attention: John W. White, Chief Propulsion Division	1
NASA-Lewis Research Center Fluid System Components Division Attention: I. I. Pinkel E. E. Bisson R. L. Johnson W. R. Loomis L. P. Ludwig M. A. Swikert T. B. Shillito		1 1 1 1 1 1 1	U. S. Army Ordnance Rock Island Arsenal Laboratory Rock Island, Illinois Attention: R. LeMar AVCOM AMSAVEGTT Mart Building 405 South 12th Street St. Louis, Missouri 63100	1
NASA Headquarters Washington, D. C. 20546 Attention: N. F. Rekos (RAP) A. J. Evans (RAD) J. Maltz		1 1 1	Attention: E. England Acrojet-General Corporation 20545 Center Ridge Road Cleveland, Ohio 44116	1
NASA-Langley Research Center Langley Station Hampton, Virginia 23365 Attention: Mark R. Nichols		1	Attention: W. L. Snapp Avco Corporation Lycoming Division Stratford, Connecticut	1
FAA Headquarters 800 Independence Avenue, S. W. Washington, D. C. Attention: J. Chavkin, SS/120 M. Lott, FS/141		1 1	Attention: R. Cuny Battelle Memorial Institute 505 King Avenue Columbus 1, Ohio Attention: C. H. Allen	1 1
Air Force Materials Laboratory Wright-Patterson Air Force Base, Ohio 45433 Attention: MANL, R. Adamczak MANE, R. Headrick & J. M. Kelble MAAE, P. House		1 1 1	Bendix Corporation Fisher Building Detroit 2, Michigan Attention: R. H. Isaacs B. F. Goodrich Company Aerospace & Defense Products Division	1
Air Force Systems Engineering Group Wright-Patterson Air Force Base, Ohio 45433 Attention: SESHS, J. L. Wilkins SEJPF, S. Prete		1 1	Troy, Ohio Attention: L. S. Blalkowski Boeing Aircraft Company 224 N. Wilkinson Dayton, Ohio 45402	1
Air Force Aero Propulsion Laboratory Wright-Patterson Air Force Base, Ohio 45433 Attention: AFAPL (APFL), K. L. Berkey & L. DeBrohum AFAPL (APTC), C. Simpson APTP, I. J. Gershon		 1 1 1	Attention: H. W. Walker Borg-Warner Corporation Roy C. Ingersoll Research Center Wolf and Algonquin Roads Des Plaines, Illinois	1 1
U. S. Naval Air Material Center Aeronautical Engine Laboratory Philadelphia 12, Pennsylvania Attention: A. L. Lockwood		1	Carbon Products Division of Union Carbide Corporation 270 Park Avenue New York, New York 10017 Attention: J. Curran	1

Semiannual Reports

Distribution List (Cont'd)
NAS3-7609

To:	Number of Copies	To:	Number of Copies
Cartiseal Corporation 3515 West Touhy Lincolnwood, Illinois Attention: R. Voltik	1	General Motors Corporation Allison Division Plant #8 Indianapolis, Indiana Attention: E. M. Deckman	1
Chicago Rawhide Manufacturing Company 1311 Elston Avenue Chicago, Illinois Attention: R. Blair	1	Hercules Powder Company, Inc. 900 Market Street Wilmington, Delaware	1
Clevite Corporation Cleveland Graphite Bronze Division 17000 St. Clair Avenue Cleveland, Ohio 44110 Attention: Thomas H. Koenig	1	Hughes Aircraft Company International Airport Station P. O. Box 90515 Los Angeles 9, California	1
Continential Aviation & Engineering 12700 Kercheval Detroit 15, Michigan Attention: A. J. Follman	1	Huyck Metals Company P. O. Box 30 45 Woodmont Road Milford, Connecticut Attention: J. I. Fisher	1
Crane Packing Company 6400 W. Oakton Street Morton Grove, Illinois Attention: Harry Tankus	1	I.I.T. Research Foundation 10 West 35th Street Chicago, Illinois 60616 Attention: Dr. Strohmeier	1
Douglas Aircraft Company Holiday Office Center 16501 Brookpark Road Cleveland, Ohio 44135 Attention: J. J. Pakiz	1	Industrial Tectonics Box 401 Hicksville, New York 11801 Attention: J. Cherubin	1
Durametallic Corporation Kalamazoo, Michigan Attention: H. Hummer	1	Kendall Refining Company Bradford, Pennsylvania Attention: F.I.I Lawrence	1
E. I. duPont de Nemours & Company 1007 Market Street Wilmington 98, Delaware Attention: G. Finn R. J. Laux A. J. Cheney	1 1 1	Koppers Company, Inc. Metal Products Division Piston Ring and Seal Department Baltimore 3, Maryland Attention: F. C. Kuchler	1
Esso Research & Engineering Company P.O. Box 51 Linden, New Jersey Attention: W. O. Taff	1	Koppers Company, Inc. Monrosville, Pennsylvania Attention: Billy D. Pfoutz	1
Fairchild Engine and Airplane Corporation Stratos Division Bay Shore, New York	1	Lockheed Aircraft Company 16501 Brookpark Road Cleveland, Ohio 44135 Attention: L. Kelly	1
Fairchild Hiller Corporation Republic Aviation Division Farmingdale, Long Island New York 11735 Attention: D. Schroeder	1	Martin Company 16501 Brookpark Road Cleveland, Ohio 44135 Attention: Z. G. Horvath	1
Franklin Institute Laboratories 20th & Parkway Philadelphia 3, Pennsylvania Attention: J. V. Carlson	1	Mechanical Technology Incorporated 968 Albany-Shaker Road Latham, New York Attention: Donald F. Wilcock	1
Garlock, Inc. Palmyra, New York 14522 Attention: E. W. Fisher	1	Metal Bellows Corporation 20977 Knapp Street Chatsworth, California Attention: Sal Artino	1
General Dynamics Corporation 16501 Brookpark Road Cleveland, Ohio 44135 Attention: George Vila	1	Midwest Research Institute 425 Volker Blvd. Kansas City 10, Missouri Attention: V. Hopkins	1
General Electric Company Advanced Engine and Technology Department Cincinnati, Ohio 45215 Attention: L. B. Venable G. J. Wile C. C. Moore H-25	1 1 1	Monsanto Chemical Company 800 North Lindbergh Blvd. St. Louis, Missouri 63166 Attention: K. McHugh R. Hatton	1 1
		Morganite, Inc. 33-02 48th Avenue Long Island City 1, New York Attention: S. A. Rokaw	1

Semiannual Reports

Distribution List (Cont'd)
NAS3-7609

To:	Number of Copies	To:	Number of Copies
North American Aviation Inc. 16501 Brookpark Road Cleveland, Ohio 44135 Attention: George Bremer	1	Southwest Research Institute 8500 Culebra Road San Antonio, Texas Attention: P. M. Ku	1
Northrop Corporation 1730 K Street N. W. Suite 903-5 Washington 6, D. C. Attention: S. W. Fowler, Jr.	1	Stanford Research Institute Menlo Park, California Attention: R. C. Fey	1
Pesco Products Division Borg-Warner Corporation 24700 N. Miles Bedford, Ohio	1	Stein Seal Company 20th Street & Indiana Avenue Philadelphia 32, Pennsylvania Attention: Dr. P. C. Stein	1
Pressure Technology Corporation of America 453 Amboy Avenue Woodbridge, New Jersey Attention: A. Dobrowsky	1	Sun Oil Company Automotive Laboratory Marcus Hook, Pennsylvania Attention: J. L. Griffith	1
Rocketdyne 6633 Canoga Avenue Canoga Park, California Attention: M. Butner	1	Union Carbide Chemicals Company Division of Union Carbide Corporation Tarrytown, New York Attention: W. H. Millott & J. C. Haaga	1
Sealol Inc. P. O. Box 2158 Providence 5, Rhode Island Attention: Justus Stevens	1	United States Graphite Company 1621 Holland Saginaw, Michigan Attention: F. F. Ruhl	1
Sinclair Refining Company 600 5th Avenue New York, New York 10020 Attention: C. W. McAllister	1	Westinghouse Electric Corporation 55 Public Square Cleveland, Ohio 44113 Attention: Lynn Powers	1
Sinclair Research Incorporated 400 E. Sibley Blvd. Harvey, Illinois Attention: M. R. Fairlie	1	Wright Aeronautical Division Curtiss-Wright Corporation 333 West 1st Street Dayton 2, Ohio Attention: S. Lombardo	1
SKF Industries, Inc. 1100 First Avenue King of Prussia, Pennsylvania Attention: L. B. Sibley	1	Pennsylvania State University Department of Chemical Engineering University Park, Pennsylvania Attention: Dr. E. E. Klaus	1
Socony Mobil Oil Company Research Department Paulsboro Laboratory Paulsboro, New Jersey Attention: E. Oberright	1	The University of Tennessee Department of Mechanical and Aerospace Eng. Knoxville, Tennessee Attention: Professor W. K. Stair	1 1